8-1-2014

Post-glacial sea-level change along the Pacific coast of North America

Dan H. Shugar
University of Washington Tacoma, dshugar@uw.edu

Ian J. Walker

Olav B. Lian

Jordan BR Eamer

Christina Neudorf

See next page for additional authors

Authors
Dan H. Shugar, Ian J. Walker, Olav B. Lian, Jordan BR Eamer, Christina Neudorf, Duncan McLaren, and Daryl Fedje

Post-glacial sea-level change along the Pacific coast of North America

Dan H. Shugar[1,*], Ian J. Walker[1], Olav B. Lian[2], Jordan B.R. Eamer[1], Christina Neudorf[2,4], Duncan McLaren[3,4], Daryl Fedje[3,4]

[1]*Coastal Erosion & Dune Dynamics Laboratory, Department of Geography, University of Victoria, Victoria, BC, Canada *dshugar@uvic.ca*
[2]*Department of Geography, University of the Fraser Valley, Abbotsford, BC, Canada*
[3]*Department of Anthropology, University of Victoria, Victoria, BC, Canada*
[4]*Hakai Beach Institute, Calvert Island, BC, Canada*

Abstract

Sea-level history since the Last Glacial Maximum on the Pacific margin of North America is complex and heterogeneous owing to regional differences in crustal deformation (neotectonics), changes in global ocean volumes (eustasy) and the depression and rebound of the Earth's crust in response to ice sheets on land (isostasy). At the last glacial maximum, the Cordilleran Ice Sheet depressed the crust over which it formed and created a raised forebulge along peripheral areas offshore. This, combined with different tectonic settings along the coast, resulted in divergent relative sea-level responses during the Holocene. For example, sea level was up to 200 m higher than present in the lower Fraser Valley region of southwest British Columbia, due largely to isostatic depression. At the same time, sea level was 150 m lower than present in Haida Gwaii, on the northern coast of British Columbia, due to the combined effects of the forebulge raising the land and lower eustatic sea level. A forebulge also developed in parts of southeast Alaska resulting in post-glacial sea levels at least 122 m

lower than present and possibly as low as 165 m. On the coasts of Washington and Oregon, as well as south-central Alaska, neotectonics and eustasy seem to have played larger roles than isostatic adjustments in controlling relative sea-level changes.

Keywords: relative sea level; isostasy, neotectonics; coastal geomorphology; Cascadia; Holocene glaciation

Table of Contents

1.0 Introduction

The northwestern coast of North America has undergone dramatic and spatially heterogeneous sea-level changes since the Last Glacial Maximum (LGM). Relative sea level (RSL) histories vary with distance from ice loading and associated factors such as time-transgressive ice retreat, diverse tectonic settings, and differential crustal responses. On the Oregon and much of Washington State's coasts, which were not glaciated, RSL history is governed primarily by eustatic sea level rise, overprinted by seismicity, with over a dozen great subduction-zone earthquakes (M 8-9) occurring throughout the Holocene. In British Columbia, the magnitudes of RSL change are greater than in southern Washington and Oregon. Further, RSL curves in British Columbia are spatially and temporally heterogeneous, owing primarily to isostatic effects. In southeast Alaska, the main driver of RSL changes has been isostasy. Parts of southeast Alaska are presently undergoing the fastest crustal uplift rates in the world (Larsen et al., 2005), due largely to extensive post-Little Ice Age (LIA) ice retreat in Glacier Bay. In contrast, the main driver of RSL change in south-central Alaska has been, and continues to be, neotectonics, due to the subduction of the Pacific Plate along the Aleutian megathrust zone.

In this paper, we provide a comprehensive survey of the extensive literature and related datasets on RSL change along the northwestern coast of North America (Figure 1). From this, we assess the main geophysical contributions to RSL dynamics throughout the region since the LGM and provide comprehensive sub-regional interpretations of how these contributions may have combined and varied from Alaska through British Columbia and Cascadia. One of our central arguments is that RSL

changes in western North America during the late Quaternary period were highly localized due to substantial differences in geophysical forcing mechanisms.

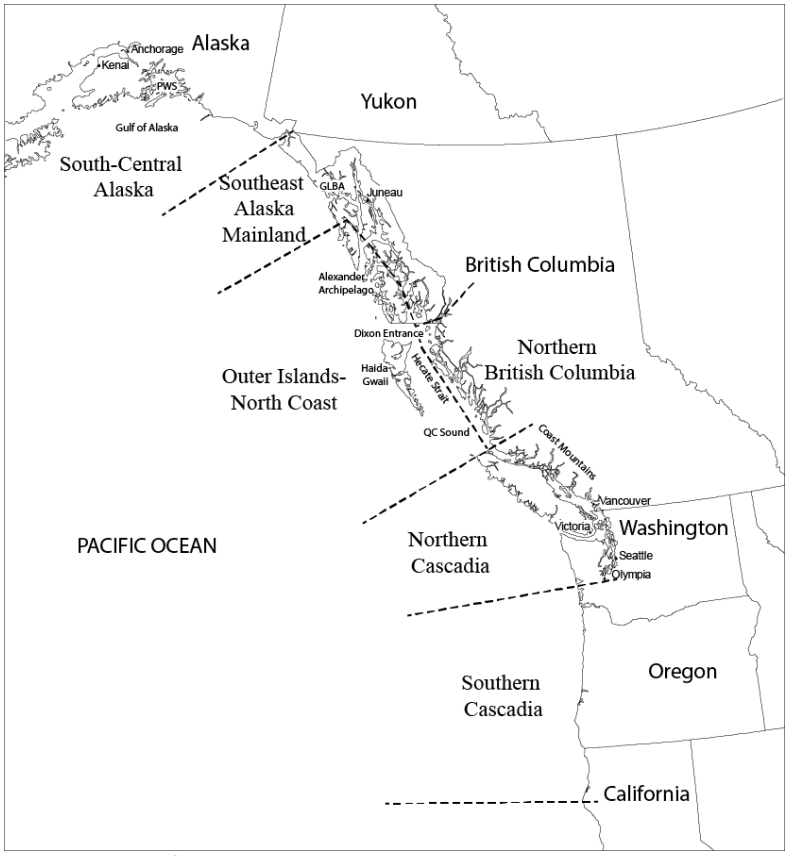

Figure 1. Map of western North America showing the sub-regions described in text. Also shown are major cities and physiographic features. Abbreviated features include QC (Queen Charlotte) Sound, GLBA (Glacier Bay), and PWS (Prince William Sound).

1.0.1 Database of sea-level points, sea-level datums and dating conventions

The database (available as a supplementary table) and the age-elevation plots presented here, include 2,191 sea-level indicators from previously published sources. Metadata for each entry includes a location and material description, latitude, longitude, sample elevation, published elevation datum, correction factor to mean sea level (msl), and a citation reference. Additionally, a radiocarbon lab identifier, published radiocarbon age, radiocarbon age 'uncorrected' (if applicable) for marine reservoir effects, median and 2σ calibrated age range are included for each sample. Many of the data were collected decades ago, and are missing important information that would facilitate assigning an 'indicative meaning', which requires both a reference water level and an indicative range (the range over which the sediment or organism was deposited or lived) (c.f. Shennan, 1986; Shennan et al., 2006; Engelhart et al., 2009). For example, many samples are described only as 'marine shells', which provides no information on the indicative range. Further, many samples of freshwater peats, shell middens, etc, represent limiting ages, as they do not show a direct relationship to tidal levels. For example, freshwater peats may have formed at approximately mean high spring tide or an some unknown height above that datum (e.g. Shennan and Horton, 2002). Instead, and for consistency, samples included in the database are assigned an 'RSL significance' of supratidal, intertidal, or marine.

Reported elevations in this paper are relative to present mean sea level. Where originally reported relative to a different datum (e.g. high tide), elevations have been converted using either the NOAA Datums website (tidesandcurrents.noaa.gov) or by employing data from the Canadian Hydrographic Service (Bodo de Lange Boom, *pers.*

131 *comm*., 2013). If not specified in the original publication, msl was assumed. Tidal ranges
132 were assumed not to have changed since the time of deposition, although previous
133 studies have argued that this is unlikely due to changes to coastline shape and
134 bathymetry (c.f. Shennan et al., 2006).
135 Calibration of published radiocarbon ages was carried out using the Calib 7.0
136 program (Stuiver et al., 2013) using the INTCAL13 radiocarbon dataset for terrestrial
137 samples and MARINE13 dataset for marine samples, with a lab error multiplier of 1.0. A
138 regional reservoir correction was applied to marine samples, based on a weighted
139 mean, ΔR, of up to the 10 nearest known-age samples within 500 km of each sample
140 (see http://calib.qub.ac.uk/marine/). Calibrated 2σ date ranges are reported as kilo
141 calendar years (ka) BP (before AD 1950).

142 ## 1.1 Causes of relative sea-level change

143 Relative sea-level changes at any location are the result of oceanic and crustal
144 factors operating at a range of spatial and temporal scales (Nelson et al., 1996b).
145 Coseismic subsidence, for example, can cause meters of RSL change in seconds, while
146 steric effects can take hundreds or thousands of years to manifest. First, we discuss the
147 main oceanic factors (eustasy, steric effects), and then the crustal factors (deformation,
148 isostasy, sedimentation) that contribute to late-Quaternary RSL changes.

149 ### *1.1.1 Eustasy*

150 Eustatic sea-level changes result from either a change in the volume of seawater,
151 or a change in the size of the ocean basins (Figure 2). Eustatic changes in sea level are
152 not uniform over the ocean basins, but vary in response to the volume of ice on land,

153 tectonic setting, sedimentation rates, and changes in seawater density (Farrell and
154 Clark, 1976).

155 During the late Quaternary, global sea level changed dramatically, rising
156 approximately 120 m over the past ~21 ka due primarily to rapid deglaciation after the
157 LGM (Fairbanks, 1989). During this time, eustatic sea-level rise was not monotonic, but
158 punctuated by several abrupt meltwater pulses (e.g. Gregoire et al., 2012).

159 Uncertainties in the limits of ice sheets at the LGM (Lambeck and Chappell, 2001)
160 hinder estimates of eustatic sea-level change, although attempts have been made to
161 model the contribution (e.g. Fleming et al., 1998; Peltier, 2002). Post-LIA eustatic
162 changes are better constrained and recent contributions of Alaskan glaciers to global
163 sea level have attracted significant attention (Larsen et al., 2005; Berthier et al., 2010).

164 ***1.1.2 Steric effects***

165 Steric effects are those related to changes in sea level resulting from thermal
166 expansion or contraction. Milne et al. (2009) argued that, although there were large
167 ocean temperature variations during deglaciation following the LGM, steric effects were
168 probably within the range of data uncertainty in most regions around the world and
169 almost certainly much smaller than eustatic and isostatic effects. The relative
170 contribution of steric effects (Figure 2) to early Holocene sea levels was probably
171 minimal (Smith et al., 2011), and likely less than to late Holocene and 20th century sea-
172 level rise. Further, steric contributions to 20th century RSL changes may have been
173 miscalculated in past studies (Domingues et al., 2008).

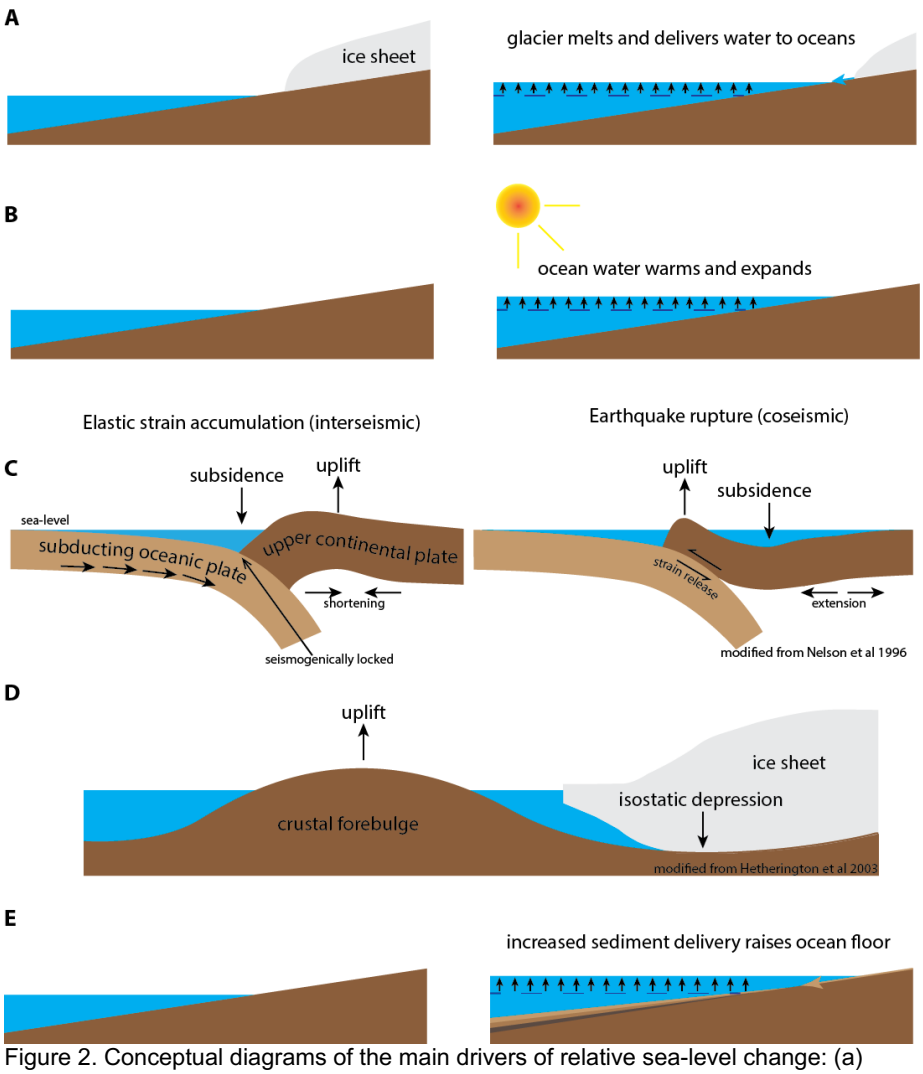

Figure 2. Conceptual diagrams of the main drivers of relative sea-level change: (a) eustasy; (b) steric expansion; (c) interseismic and coseismic strain; (d) isostatic depression and forebulge development; and (e) sedimentation.

1.1.3 Crustal deformation (neotectonics)

Atwater (1987) provided the first evidence for sudden neotectonic submergence of Holocene coastal forests and grasslands in Washington State, and suggested that great (magnitude 8 or 9) megathrust earthquakes over the Holocene originated from the Cascadia subduction zone, and that RSL variations were punctuated by sudden tectonic subsidence during this time. Coastal coseismic subsidence and uplift resulting from subduction zone tectonics have been documented in Alaska (Combellick, 1991; Hamilton and Shennan, 2005a), Cascadia (Atwater and Yamaguchi, 1991; Nelson et al., 1996b; Leonard et al., 2004), Chile (Plafker and Savage, 1970; Cisternas et al., 2005), and Japan (Thatcher, 1984; Savage and Thatcher, 1992).

Patterns of land and sea-level movements accompanying Cascadian and Alaskan earthquakes, described as an “earthquake deformation cycle” (e.g. Long and Shennan, 1994; Hamilton and Shennan, 2005b), consist of gradual interseismic strain accumulation lasting centuries followed by sudden coseismic deformation during plate-boundary rupture. Crustal deformation can have two repercussions for RSL (Figure 2). Between earthquakes, uplift (and RSL regression) occurs landward of the locked zone (zone of maximum convergent-strain accumulation), while subsidence (and RSL rise and potential transgression) occurs seaward of it. During an earthquake, the inverse occurs whereby coseismic uplift seaward of the locked zone results, causing a certain amount of RSL drop, whereas subsidence and RSL rise occurs landward of the locked zone (e.g. Nelson, 2007).

Monitoring of modern land motions, measured using short-term tide gauges, repeat leveling, and GPS, forms the basis of efforts to model long-term plate boundary interseismic strain (Long and Shennan, 1998; Rogers and Dragert, 2003). For instance, Hyndman and Wang (1995) showed that much of the Cascadia subduction zone (see Section 2.1, below) was experiencing crustal uplift with maximum uplift rates occurring closer to the coast. These results are independent of the eustatic or regional sea-level changes.

1.1.4 Isostasy

When ice sheets melt, the resulting RSL changes are spatially heterogeneous due in part to differential responses of the crust to ice unloading (Figure 2). At the maximum of the last (Fraser) glaciation, the entire glaciated Cordillera was isostatically depressed, although exact magnitudes of depression are unknown (Clague, 1989a). Assuming approximately 100 m of eustatic sea-level lowering at the time the highest shorelines were formed in southwest British Columbia during deglaciation for example, Clague and James (2002) proposed that local isostatic depression was at least 300 m to as much as 500 m. In contrast, evidence for an offshore crustal forebulge, and associated sea-level low stands exists on Haida Gwaii (formerly the Queen Charlotte Islands) and southwestern Alexander Archipelago in southeast Alaska (Clague et al., 1982a; Fedje et al., 2005; Baichtal et al., 2012).

1.1.5 Sedimentation

Sedimentation effects can cause RSL to increase (by sediment compaction) or decrease (by deposition and accumulation of nearshore sediments). Some of the most

222 rapid sediment transfers between land and sea are associated with tsunamis (e.g.
223 Atwater and Yamaguchi, 1991), although inputs from large rivers (Williams and Roberts,
224 1989; Clague et al., 1991; Goodbred and Kuehl, 2000), glaciers (Clague, 1976) and
225 anthropogenic influences (Mazzotti et al., 2009) can also result in large local sediment
226 fluxes (Figure 2).
227 Contemporary sea-level rise in the Fraser River delta in southwest British
228 Columbia for example, is exacerbated by anthropogenic sediment consolidation in
229 response to urban development and resulting local ground subsidence rates ranging
230 from -3 to -8 mm a^{-1} (Mazzotti et al., 2009). Elsewhere, other authors (e.g. Horton and
231 Shennan, 2009; Nittrouer et al., 2012; Nittrouer and Viparelli, 2014) have observed
232 similar RSL adjustments due to sedimentation effects. Compared with other drivers of
233 RSL change, however, the effects of sedimentation are highly localized and, are
234 probably a relatively minor contributor to overall RSL change since the LGM.

235 ## 2.0 Regional setting

236 This study examines fluctuations in RSL over the late Quaternary along the
237 northeastern coast of the Pacific Ocean from southern Cascadia (northern California,
238 Oregon, Washington), through British Columbia, and into southern Alaska (Figure 1).
239 This broad region is diverse in physiography, tectonics, crustal rheology, and glacial ice
240 loading and retreat history. For the purposes of this study, the region is partitioned into
241 five sub-regions, each defined by a combination of political boundaries and geophysical
242 conditions. As tectonic activity and related co- and interseismic RSL adjustments vary
243 markedly across these regions, we preface the general overview of the sub-regions with
244 a review of the broader tectonic regimes that underlie them. Further, this review and

subsequent RSL trend analyses are restricted to the regions seaward of the fjord heads on the mainland and landward of the edge of the continental shelf.

2.1 Regional tectonic regime

The coastal regions of northwestern North America are characterized by several major tectonic regimes that have played notable roles in regional sea level histories (Figure 3). From south to north, these include (1) the Cascadia subduction zone; (2) the predominantly strike-slip Queen Charlotte-Fairweather fault zone; (3) a transition zone between strike-slip and underthrust motion in the eastern Gulf of Alaska; and (4) the Alaska-Aleutian megathrust subduction zone in south-central Alaska and the Aleutian Islands (Nishenko and Jacob, 1990; Freymueller et al., 2008).

The present tectonic regime of Cascadia is controlled mainly by the motions of the Pacific, North American and Juan de Fuca plates (Figure 3). In addition, the smaller Explorer plate on the north end of the Juan de Fuca plate, and the Gorda plate on the south end, may be moving as independent units (Mazzotti et al., 2003). The southern limit of the Cascadian subduction zone occurs where the Juan de Fuca plate is intersected by the San Andreas and Medocino strike-slip faults at the Mendocino triple junction located just offshore of northern California. The oceanic Juan de Fuca and Gorda plates are moving northeasterly at a relative rate of about 40 mm a^{-1} and are colliding with, and being subducted beneath, the continental North American plate (Hyndman et al., 1990; Komar et al., 2011).

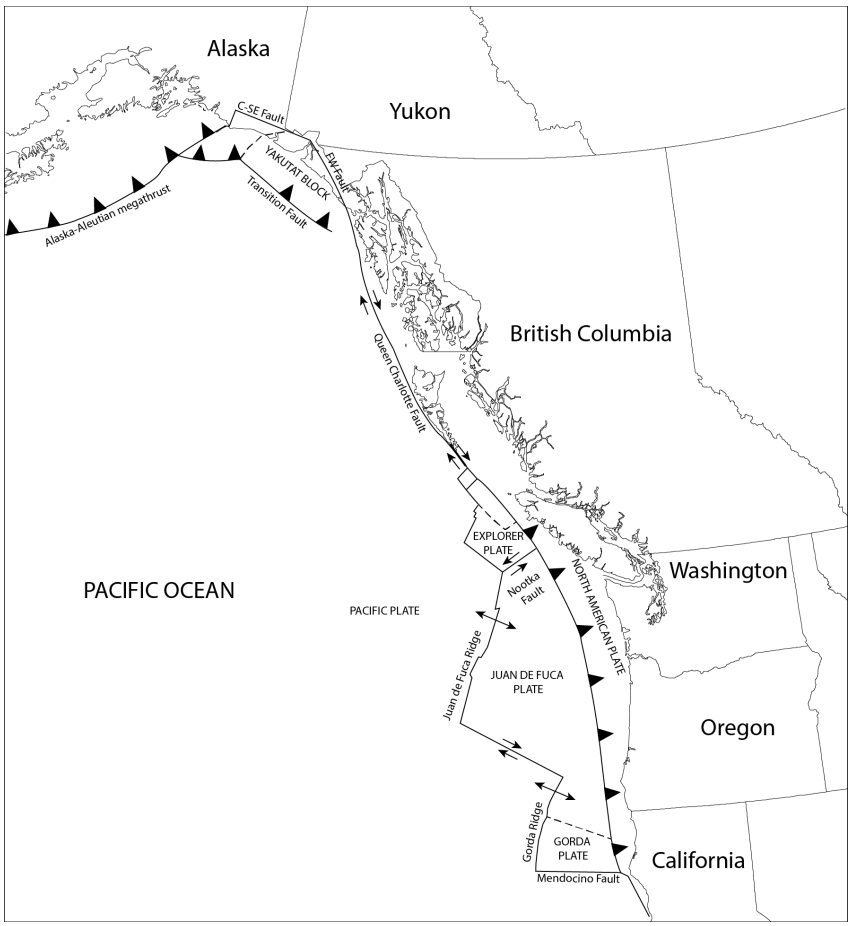

Figure 3. Map of the tectonic setting of western North America. Abbreviated faults include C-SE (Chugach-St. Elias), and FW (Fairweather) faults.

Hyndman and Wang (1995) showed that much of the Cascadia subduction zone was experiencing crustal uplift of between 0 and 5 mm a^{-1} with maximum uplift rates occurring closer to the coast. These results are independent of the eustatic or regional sea-level changes. Similarly, Mazzotti et al. (2008) reported upward vertical velocities of between 1 to 3 mm a^{-1} for coastal sites throughout the Cascadian region, but did not

attempt to partition the signal into interseismic strain and isostatic rebound. Inland sites tended towards lower vertical velocities, with slight subsidence in some cases (to -1 mm a^{-1}).

The Pacific and North American plates and the Winona block also form a triple junction at the north end of Vancouver Island, which serves as the northern boundary of the Cascadia subduction zone (Clague, 1989a). To the north of the Cascadia subduction zone, displacements along the dextral Queen Charlotte-Fairweather fault average between 43 to 55 mm a^{-1} (Clague, 1989a; Elliott et al., 2010). Following the 2012 Haida Gwaii earthquake, Szeliga (2013) argued that the northern end of subduction along the Cascadia margin may need to be redefined, as the primarily strike-slip Queen Charlotte Fault has a smaller component of convergence. Early GPS data from that earthquake indicate a meter of coseismic displacement toward the rupture, followed by more than 1 mm d^{-1} of postseismic strain (James et al., 2013). The north end of the Queen Charlotte fault is affected by the motion of the Yakutat Block (see below) that causes the Queen Charlotte fault to rotate clockwise (e.g. Elliott et al., 2010), and subduct beneath the North American plate (e.g. Lay et al., 2013). The Queen Charlotte-Fairweather fault complex continues north into southeast Alaska, ending near Yakutat Bay (Figure 3).

The Yakutat block is a wedge-shaped, allochthonous terrane in the process of accreting onto the North American plate. It is bounded by the Fairweather fault (east), the Transition fault (south), and the Chugach-St. Elias fault (north) and it is moving between 45 to 50 mm a^{-1} north-northwest (Freymueller et al., 2002; 2008; Elliott et al., 2010). West of the Yakutat Block, the Pacific plate is subducting under the North

American plate along the Alaska-Aleutian megathrust at a rate of about 57 mm a^{-1} (Cohen and Freymueller, 2004). South-central Alaska is tectonically complex and tectonic implications for RSL changes are appreciable.

2.2 Southern Cascadia sub-region

The southernmost physiographic sub-region, termed southern Cascadia, includes the unglaciated coastal regions of the Cascadia subduction zone, which extend from northern California (north of Cape Mendocino) to south of Olympia, Washington at about 47°N (Figure 1). The northern limit of this region at Olympia was the southernmost extent of the Cordilleran Ice Sheet (Armstrong, 1981; Dethier et al., 1995). The rationale for delimiting this region was to identify a region with a broadly similar tectonic setting along the Cascadian subduction zone north of the Mendocino triple junction that was also not as influenced by notable glacio-isostatic effects during the LGM and subsequent glacial retreat as in northern Cascadia.

The coastal region of southern Cascadia is bereft of fjords and islands, which are common along the formerly glaciated coast further north. Instead, the coast of southern Cascadia is characterized by mostly sandy beaches, typically backed by sea cliffs eroded into Paleogene and Neogene mudstones and siltstones, which are capped by Pleistocene terrace and fan deposits (Allan et al., 2003). Low-lying stretches of the Oregon and southern Washington coasts are backed by extensive sand dune complexes and barrier spits. In Oregon, Clemens and Komar (1988) found that present sources of sediment to the coast are insufficient to supply the beaches and that the sand must have been carried onshore by beach migration under rising relative sea levels at the end of the Pleistocene glaciation.

2.3 Northern Cascadia sub-region

The northern Cascadia sub-region extends from the southernmost limit of the Cordilleran Ice Sheet at the LGM near Olympia, Washington, to the north end of Vancouver Island at about 51°N (Figure 1). Thus, this sub-region represents most of the glaciated extent of the Cascadia Subduction zone, as well as the northern limit of plate rupture resulting from the AD 1700 subduction earthquake (Benson et al., 1999). The region includes Puget Sound, the Olympic Peninsula, the lower Fraser Valley, Vancouver Island, and the fjords and channels at the periphery of the heavily glaciated mainland Coast Mountains.

Typically, the crystalline plutonic rocks along the mainland coast of northern Cascadia are resistant to erosion and support steep slopes and rugged topography. Major joints and faults characterize much of the coast, while glacially-carved fjords, extending up to 150 km inland, are common (Clague, 1989a; Church and Ryder, 2010). Much of the mainland coast in this region is protected from the open Pacific Ocean by Vancouver Island. Within the Strait of Georgia, which lies between Vancouver Island and the mainland, are the smaller Gulf Islands (Canada) and San Juan Islands (USA). Several of these islands are drumlinoid features capped by outwash “Quadra” sands (Clague, 1976). The geomorphology and sedimentology of these islands record the timing and paleo-flow direction of advance phase ice of the Fraser Glaciation into and across the Strait of Georgia and Puget Sound between about 34.1 to 31.4 and 19.1 to 17.2 ka BP (Clague, 1975).

2.4 Northern British Columbia sub-region

The northern British Columbia sub-region extends from northern Vancouver Island to the US-Canada border with Alaska at Dixon Entrance, including the mainland and islands of the inner coast (Figure 1). The tectonic setting of northern British Columbia is very different from southern British Columbia, being primarily characterized by the strike-slip Queen Charlotte fault as opposed to the Cascadia subduction zone. To date, no studies have documented RSL fluctuations due to tectonic factors in the northern British Columbia sub-region. Although both southern and northern British Columbia sub-regions were heavily glaciated during LGM, the RSL response differed markedly.

The physiography of the northern coast of British Columbia is similar to that of the southern coast with high peaks, steep slopes, and deep fjords. The Coast Mountains, as in southern British Columbia, consist mainly of granitic igneous rocks, but metamorphic, volcanic and sedimentary rocks are also common. The northern British Columbia coast is currently glaciated, although contains fewer large ice caps than the south Coast Mountains or southeast Alaska, to the north.

2.5 Outer Islands-North Coast sub-region

The outer islands-north coast sub-region comprises the Queen Charlotte Basin (Hecate Strait and Queen Charlotte Sound), Cook Bank, Haida Gwaii and the outer islands of the Alexander Archipelago south of Chichagof Island and west of Clarence Strait (Figure 1). The outer islands-north coast sub-region is situated along the Queen Charlotte fault.

Haida Gwaii (known formerly as the Queen Charlotte Islands) is a large archipelago of about 150 islands composed mainly of metamorphosed volcanic and

sedimentary rocks (Clague, 2003) located more than 80 km west of the mainland on the edge of the continental shelf. The Quaternary history of Haida Gwaii differs distinctly from the mainland British Columbia coast in terms of the thickness and extent of ice cover at the LGM and fluctuations in RSL in response to complex glacio-isostatic effects. The Argonaut Plain (also known as the Naikoon Peninsula) on the northeastern coast of Haida Gwaii is one of few extensive flat, low coastal plains in northern coastal British Columbia. It consists of a thick sequence of glacial outwash sediments deposited by streams that drained glaciers on the islands during the late Pleistocene (Clague, 1989b), and was reworked by littoral and aeolian processes during a late-Holocene RSL regression, leaving a series of relict shorelines and sand dunes (Wolfe et al., 2008). Prior to this, portions of the terrain on or near the islands may have provided a glacial refugium during LGM (e.g. Warner et al., 1982; Byun et al., 1997; Reimchen and Byun, 2005) when RSL was significantly lower. The southwestern islands of the Alexander Archipelago, including Baranof and Prince of Wales, as well as many smaller islands, may also have provided a glacial refugium during the LGM (Heaton et al., 1996).

2.6 Southeast Alaska Mainland sub-region

The southeast Alaska mainland sub-region encompasses the mainland and inner islands of southeast Alaska, including Revillagigedo, Kupreanof, and Admiralty islands, as well as Chichagof Island, Icy Strait, Glacier Bay, and the coast north to Yakutat Bay near where the Fairweather Fault ends (Figures 1, 2). Like much of northern British Columbia, this sub-region consists of steep, high mountains, glacially scoured islands, and deep fjords. Large glaciers occupy many valleys, and are presently thinning at rates up to 10 m a^{-1} (Larsen et al., 2005; Berthier et al., 2010). Glacier Bay is currently

experiencing some of the fastest uplift rates in the world (~30 mm a^{-1}), primarily due to the collapse of the Glacier Bay Icefield following the LIA (Motyka, 2003; Larsen et al., 2005). Unlike coastal regions in south-central Alaska to the north, large islands protect much of the mainland coast of southeast Alaska. Most shorelines are bedrock-controlled, with rocky headlands that protect relatively small, embayed beaches. Sediments on these beaches record a legacy of repeated glaciations (Mann and Streveler, 2008).

2.7 South-Central Alaska sub-region

The south-central Alaska sub-region extends from Yakutat Bay to the Cook Inlet region near Anchorage and the Kenai Peninsula (Figure 1). Like the southeast Alaska mainland sub-region, south-central Alaska is heavily glaciated, but differs in terms of tectonic regime. The outer coast of this region is generally characterized by high wave energy and is backed closely by steep, rugged, and heavily glaciated mountain ranges (Kenai, Chugach, and Wrangell). Aside from Cook Inlet and Prince William Sound, which are protected by numerous rocky islands, most of the south-central Alaskan coastline is exposed. West of Hinchinbrook Island in Prince William Sound, the coastline is primarily rocky, while eastward it is mostly composed of sand and gravel deposits originating from coastal glaciers and the Copper River (Mann and Hamilton, 1995).

3.0 Late-glacial and post-glacial sea levels

In this section, we describe the geological, geomorphic and anthropological evidence for RSL since the LGM. Discussion of the causes of these fluctuations is provided in the following section.

3.1 Southern Cascadia

Little empirical evidence exists for early post-glacial shorelines in southern Cascadia. Glacio-isostatic contributions were much less in southern Cascadia than in areas depressed by the Cordilleran Ice Sheet (Dalrymple et al., 2012), but were still an influence on RSL. Recent modeling efforts by Clark and Mitrovica (2011) found that, on the Washington and Oregon continental shelf, RSL at the LGM was about -120 m due mostly to eustatic lowering (Figure 4). Glacio-isostatic adjustment (GIA) modeling suggested that RSL has never risen above present sea level throughout the Holocene near the mouth of the Columbia River at Long Beach, Washington. Instead, it rose from nearly -100 m at about 18 ka BP, to approximately -75 m around 16.5 ka BP as the sea flooded isostatically depressed land, then dropped back to -100 m around 13 ka BP in response to glacio-isostatic uplift. According to the GIA modeling, RSL appears to have risen slowly to the present since about 13 ka BP (Dalrymple et al., 2012).

The late-Holocene sea-level history of southern Cascadia is better constrained than early postglacial times (Figure 4). Over the past 4 ka, Long and Shennan (1998) inferred near linear rises in RSL of about 3 m and 5 m up to present datum in Washington and Oregon, respectively, and interpreted this as a response to a north-south decline in the rate of isostatic rebound. This regular and relatively recent decline

430 is different from that interpreted for northern Cascadia, where rebound was thought to
431 be complete by the early Holocene (e.g. Mathews et al., 1970; James et al., 2009b). At
432 Coos Bay, Oregon, however, Nelson et al. (1996a) argued for a more punctuated RSL
433 rise in the mid- to late-Holocene. They suggested that ten peat-mud couplets dating
434 since 4.8 to 4.5 ka BP represent either instantaneous coseismic subsidence or rapid
435 RSL rise (i.e., within a few years or decades) resulting from sudden breaching of tide-
436 restricting bars or an abrupt change in the shape of an estuary. In the past millennia,
437 only one peat-mud couplet, representing the AD 1700 earthquake, was identified by
438 Nelson et al. (1996a). At Alsea Bay, Oregon, Nelson (2007) argued that interbedded
439 soils and tidal muds resulted from slow eustatic sea-level rise, tidal sedimentation, and
440 sediment compaction over the last millennium, rather than unrecovered coseismic
441 subsidence (Figure 4).
442 Using tide gauge records, Komar et al. (2011) showed that parts of northern
443 California and the southern third of the Oregon coast are currently rising faster due to
444 tectonic uplift than the regional eustatic rise in sea level (+2.28 mm a^{-1}), resulting in an
445 emergent coast. In contrast, most of Oregon between Coos Bay and Seaside are
446 submergent and experiencing sea-level transgression. Humboldt Bay, CA, is the only
447 area along the Pacific Northwest coast where land elevation is dropping (RSL +5.3 mm
448 a^{-1}) as stress accumulates between the locked tectonic plates. Humboldt Bay is
449 significantly closer to the offshore subduction zone than are the other tide-gauge sites
450 studied by Komar et al. (2011). During periods when the plates are locked, as they are
451 now inferred to be, the proximity of Humboldt Bay to the subduction zone results in
452 deformation and down-warping of the seaward edge of the continent, causing

453 subsidence at this tide-gauge site. Komar et al. (2011) ascribe the differing RSL trends
454 to the complex tectonics of the region – the southern part of Oregon being strongly
455 affected by the subduction of the Gorda Plate under the North American plate.

456 **3.2 Northern Cascadia**

457 Although the Late Wisconsin Cordilleran Ice Sheet began to develop between
458 about 34.1 and 27.4 ka BP, it did not achieve its maximum extent in northwestern
459 Washington until much later (Clague, 1989a) and parts of Vancouver Island were ice-
460 free until later still (Howes, 1983). On western Vancouver Island, Ward et al. (2003)
461 suggest that ice cover on the outer coast was brief, lasting only from about 18.7 to 16.3
462 ka BP. Glaciers with sources in British Columbia's southern Coast Mountains and on
463 Vancouver Island coalesced to produce a piedmont lobe that flowed south into the
464 Puget Lowlands of northern Washington reaching the Seattle area about 17.4 ka BP
465 (Porter and Swanson, 1998) and its maximum extent south of Olympia about 17 ka BP
466 (Hicock and Armstrong, 1985; Porter and Swanson, 1998; Clague and James, 2002). At
467 the LGM, the Puget Lobe was more than 1,000 m thick in the vicinity of Seattle
468 (Easterbrook, 1963; Porter and Swanson, 1998). Some evidence suggests multiple
469 oscillations of the Puget Lobe at the end of the Pleistocene (Clague et al., 1997;
470 Kovanen and Easterbrook, 2002).

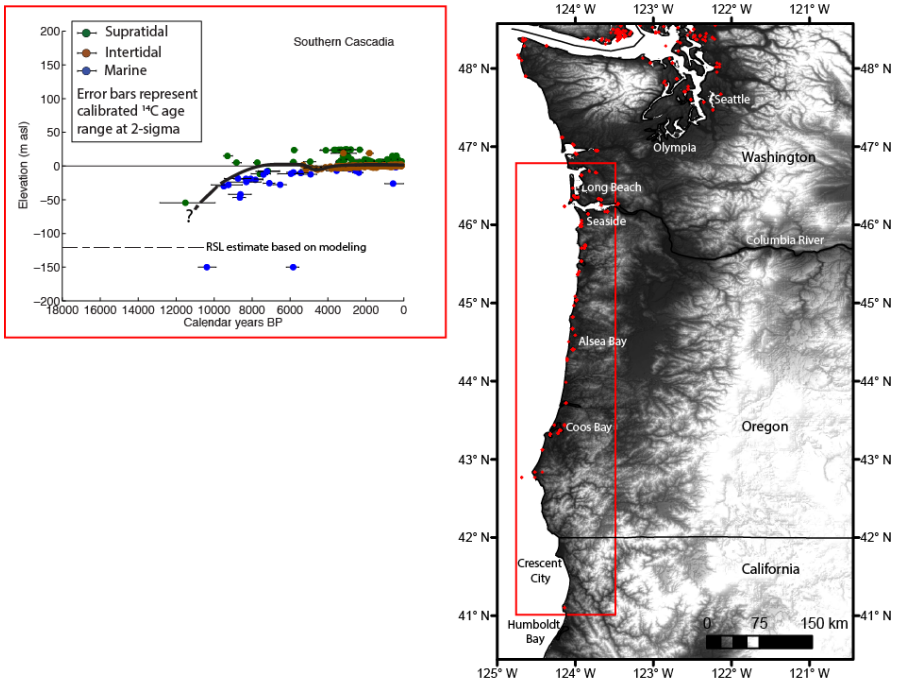

Figure 4. Relative sea level curve for the southern Cascadia sub-region.

Comment [DS1]: Note to editor and reviewers that the figure has been updated with a dashed line to reflect the modeling work of Clark and Mitrovica (2011).

The decay of the Puget lobe was extremely rapid, facilitated by calving into proglacial lakes and eventually, the Pacific Ocean. Its terminus retreated 100 km north of Seattle within 200 to 300 years of the LGM. By about 15.7 ka BP, areas that are now occupied by Vancouver and Victoria, British Columbia, had become ice-free (Clague and James, 2002). As the ice thinned and retreated, the ocean flooded isostatically depressed lowlands. In general, the relict marine limits of this transgression are highest on the mainland coast, up to approximately +200 m amsl east of Vancouver, British Columbia, prior to 13.5 ka BP (Figure 5) (Clague, 1981), and decreased to the west and southwest due to lesser glacio-isotastic depression further from the center of the ice

mass. The marine limit is about +158 m amsl at the US/Canada border, +40 m amsl at Everett, Washington, (see Figure 3, Dethier et al., 1995) and +50 m amsl at Tofino on the west side of Vancouver Island (Valentine, 1971; Clague, 1989a). The marine highstands in Washington date from 16.2 to 12.1 ka BP (Dethier et al., 1995) (Figure 6). The presence of fish bones in the Port Eliza cave (+85 m amsl) north of Tofino, indicate that RSL was close to the cave between 22.1 and 19.2 ka BP, prior to the LGM (Ward et al., 2003). An anomalously high marine limit of +180 m amsl may also exist near Deming (Easterbrook, 1963), northeast of Bellingham, Washington, although this finding is disputed (c.f. Dethier et al., 1995).

Several authors (Easterbrook, 1963; Mathews et al., 1970) have argued for a second marine transgression in southwest British Columbia and northwestern Washington during the Sumas stade 13.4 to 11.7 ka BP. Clague (1981), however, argued for a single transgression, suggesting that the sediments described by Easterbrook (1963) and Mathews et al. (1970) were probably not marine in origin. In addition, James et al. (2002) pointed out that the Sumas advance was neither thick, nor extensive enough to produce 100 m or more of isostatic depression as suggested by Easterbrook (1963), which implies that the marine sediments described are probably not marine, or at least not *in situ*. Mathews et al. (1970) themselves even cast doubt on their own dual-transgression chronology, by describing uninterrupted terrestrial conditions 105 m amsl above present sea level at Sedro Wooley, south of Bellingham, from 16.3 to 14.2 ka BP to the present.

Rapid deglaciation at the periphery of the Cordilleran Ice Sheet triggered swift isostatic adjustments and concomitant drops in RSL in northern Cascadia (Mathews et

al., 1970; Dethier et al., 1995; James et al., 2009b). Isostatic uplift was spatially heterogeneous along the British Columbia coast such that regions that were deglaciated first rebounded earlier than areas that were deglaciated later. In the Fraser Lowland near Vancouver (Figure 5), RSL fell rapidly from about +175 m amsl (13.9 to 13.5 ka BP) to below +60 m amsl (13.5 to 13.1 ka BP) (James et al., 2002) and continued regressing until it became relatively stable and below -11 m amsl between 8.8 and 7.9 ka BP, which allowed peat to accumulate below present sea level (Clague et al., 1982a). A marine transgression triggered aggradation of the Fraser River floodplain, depositing 5 m of marine silts above the peats by 6.6 ka BP (dated by the presence of layer of Mazama tephra), the upper surface of which approached present datum between 6.4 and 5.5 ka BP (Clague et al., 1982a). Based on GIA modeling constrained by RSL field data, James et al. (2009b) argue that isostatic rebound in southwest British Columbia was mostly complete within 1,000 to 2,000 years of deglaciation and present vertical crustal motions are on the order of a few tenths of a millimeter per year.

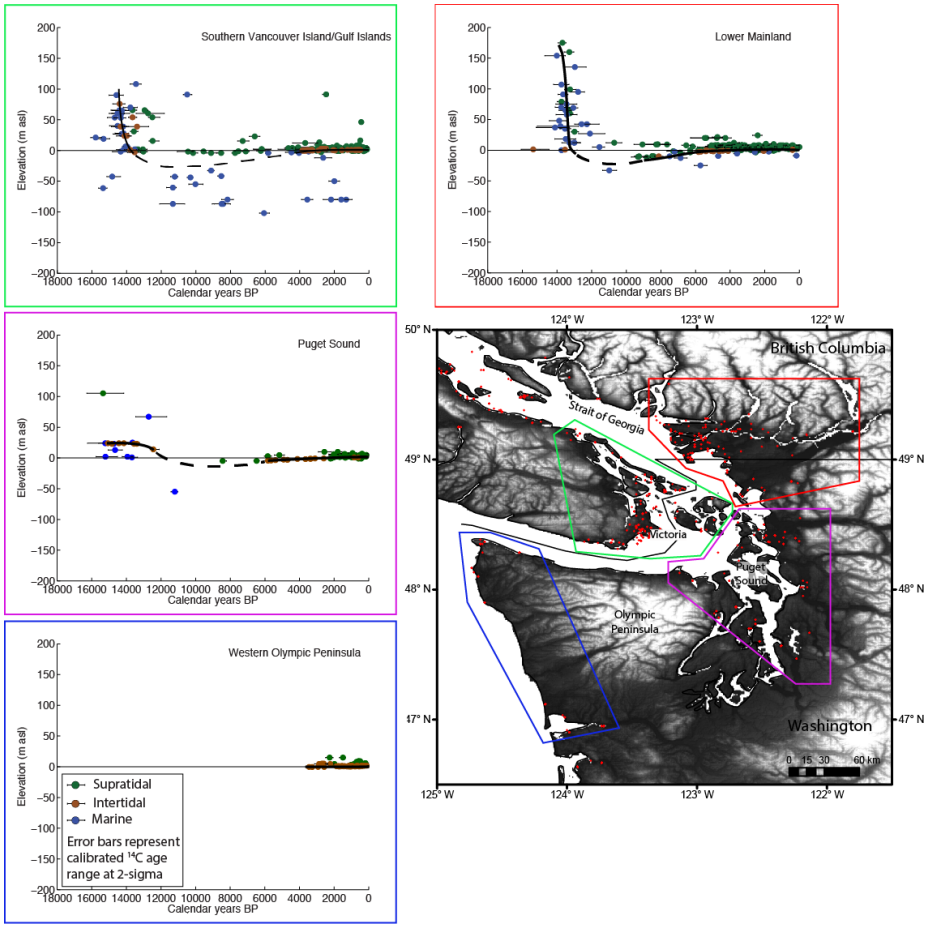

Figure 5. Relative sea level curves for part of the northern Cascadia sub-region. Shown are the Lower Mainland and Fraser Valley, southern Vancouver Island, Puget Sound and Olympic Peninsula.

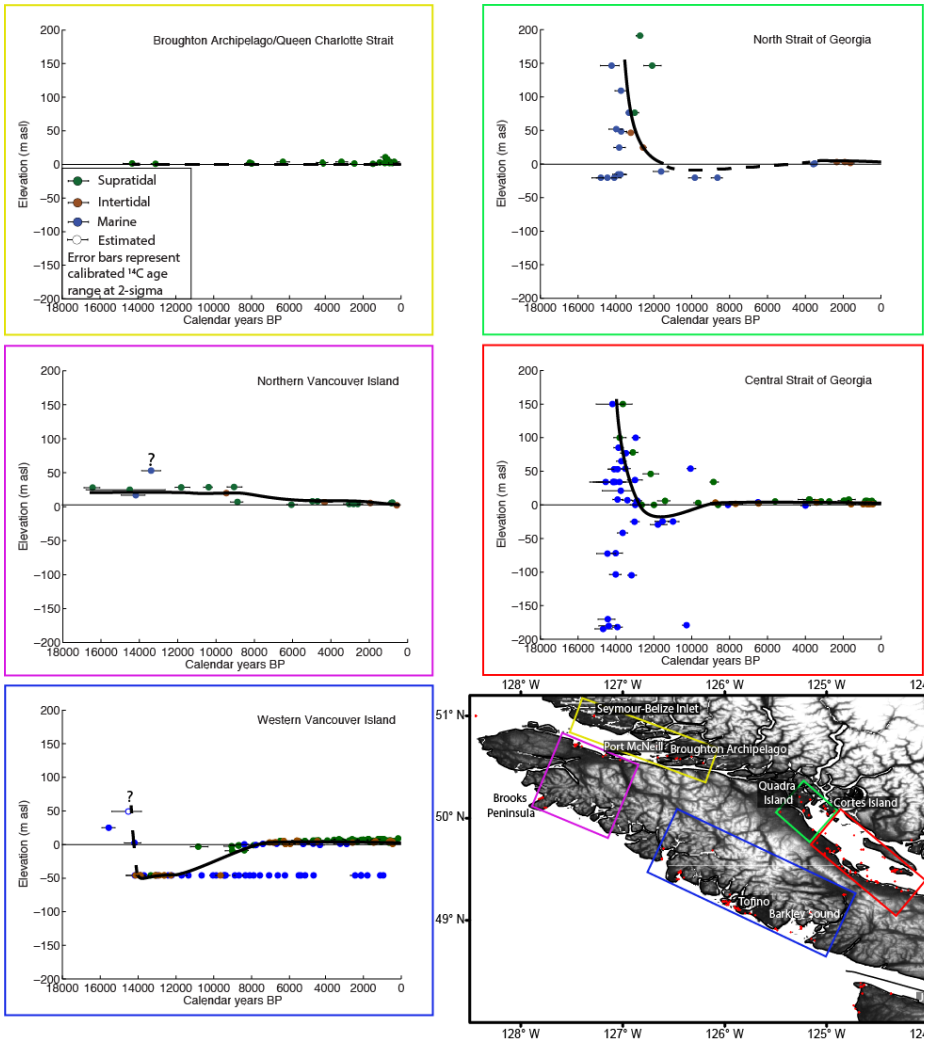

Figure 6. Relative sea level curve for part of the northern Cascadia sub-region. Shown are central and northern Vancouver Island, and mainland British Columbia.

At Victoria on southern Vancouver Island, RSL fell from its high stand of about +76 m amsl approximately 14.8 to 14.1 ka BP, to below present sea level soon after 13.4 ka

BP and reached a low stand between -30 m amsl (James et al., 2009a) and -50 m amsl (Linden and Schurer, 1988) by about 11 ka BP (Figure 5). RSL in the region was lower than present until after 6 ka BP (Clague, 1981) and probably as late as 2.0 to 1.9 ka BP (Figure 5) (Fedje et al., 2009; James et al., 2009a).

Further away from the thicker portions of the Cordilleran Ice Sheet, RSL patterns were similar but occurred with a different timing. For instance, on the northern Gulf Islands and adjacent eastern Vancouver Island in the central Strait of Georgia, where the Cordilleran Ice Sheet was present longer, RSL dropped from +150 m amsl at about 15 to 13.6 ka BP to below present datum around 12.9 to 12.7 ka BP, before reaching a low stand of about -15 m amsl by about 11.9 to 11.2 ka BP. RSL remained below present until about 8.4 to 8.3 ka BP (Hutchinson et al., 2004), after which it rose to below +4 m amsl before falling slowly to the modern datum (Figure 6). Further north on Quadra and Cortes islands in the northern Strait of Georgia, RSL dropped from above +146 m amsl after 13.8 ka BP to +46 m amsl by 13.4 to 12.9 ka BP (James et al., 2005). A low stand in the northern Strait of Georgia has not been identified, although James et al. (2005; 2009a) suggested that a low stand a few meters below present was probably reached prior to 10 ka BP. They argue that after 5 ka BP, RSL rose to, or slightly below +1.5 m amsl by 2 ka BP. From 2 ka BP to the present, RSL dropped to its present level (Figure 6) (James et al., 2005). Further still at Port McNeill on northeast Vancouver Island, marine shells at +53 m amsl record a high stand around 13.9 to 12.9 ka BP (Howes, 1983) (Figure 6).

To date, little information exists to conclusively date a post-glacial marine high stand on the west coast of Vancouver Island, although undated glaciomarine sediments

555 at Tofino (+50 m amsl) may have been deposited around 14.7 to 13.9 ka BP
556 (Bobrowsky and Clague, 1992), and strandlines at +20 m amsl on the Brooks Peninsula
557 on northwest Vancouver Island were probably formed prior to between 16.8 and 12.6 ka
558 BP (Howes, 1981, 1997). In Barkley Sound, on western Vancouver Island, Dallimore et
559 al. (2008) inferred a rapid drop in RSL to a low stand of below -46 m amsl by 13.5 to
560 13.2 ka BP, followed by a transgression starting about 11.3 ka BP until about 5.5 ka BP
561 when it stabilized at a few meters above present (Figure 6). RSL has been falling slowly
562 here since, most likely due to crustal uplift (Dallimore et al., 2008). Immediately to the
563 north at Clayoquot Sound near Tofino, Friele and Hutchinson (1993) documented a
564 gradual rise in RSL from a Holocene low stand, estimated to be below -3 m amsl prior to
565 9 ka BP. The transgression culminated in a still-stand between 6.4 to 5.3 ka BP, when
566 mean sea level was 5 to 6 m higher than present. Relative sea levels then fell to +2 m
567 amsl by 2.7 ka BP and little is known about RSL trends in Clayoquot Sound since
568 around 2 ka BP (Figure 5). Historic tide gauge and GPS data show that the Tofino
569 region is presently emergent (+2.6 mm a^{-1}) (Mazzotti et al., 2008) and shorelines in the
570 region are prograding at relatively rapid rates (0.2 to 1.1 m a^{-1}) (Heathfield and Walker,
571 2011).
572 Friele and Hutchinson (1993) ascribe the Holocene submergence-emergence
573 history on central western Vancouver Island to tectonic uplift along the North American
574 plate margin. On western and northwestern Vancouver Island near the northern
575 boundary of the subducting Juan de Fuca plate, Benson et al. (1999) described
576 stratigraphy recording 0.2 to 1.6 m of coseismic submergence due to the AD 1700
577 earthquake, followed by 1.1 m of subsequent emergence. They argue that plate rupture

during the last great Cascadia earthquake probably did not extend north of central Vancouver Island.

In the Seymour-Belize Inlet, about 40 km east of the northern tip of Vancouver Island, and the Broughton Archipelago to the southeast, Holocene RSL fluctuations are much more subtle than elsewhere in the northern Cascadia subregion. Roe et al. (2013) inferred a drop from about +2.5 m amsl around 14 ka BP to +1 m amsl by 13.2 to 13 ka BP followed by fluctuations between 0 and 1 m amsl for most of the Holocene (Figure 6). In the Broughton Archipelago, RSL was within a few meters of the present datum for the entire Holocene.

3.3 Northern British Columbia

Late Quaternary RSL trends in this region differ significantly from those on the outer coast, at Haida Gwaii and in the Alexander Archipelago in southeast Alaska (see below). In fjords on the central coast near Bella Coola, British Columbia, Retherford (1970) identified undated marine sediments at +230, +160, and +70 m amsl, and suggested that these elevations represented stable RSL stands. The undated late Pleistocene marine limit at Kitimat, which lies ~100 km inland from the coast of northern British Columbia, is approximately +200 m amsl (Figure 7). RSL regression was rapid to +98 m amsl by 11.1 to 10.2 ka BP, to above +37 m amsl by 9.8 to 9.7 ka BP, and above +11 m amsl by 10.5 to 9.5 ka BP (Figure 7) (Clague, 1981, 1984).

At Terrace, which lies ~50 km north of Kitimat and about 160 km from the outer coast, marine shells have been described ranging in elevation from +64 to +170 m amsl, the highest of which were deposited around 11.2 to 10.3 ka BP (Clague, 1984). Near Prince Rupert on the coast, west of Kitimat and Terrace, RSL was approximately

+52 m amsl at 15 to 13.7 ka BP (Fedje et al., 2005), before regressing to approximately +15 m amsl by 14 to 13.6 ka BP (Figure 7) (Clague, 1984). Since then, RSL has dropped slowly and likely been slightly below present, rising to the present datum in the late Holocene (Clague, 1984).

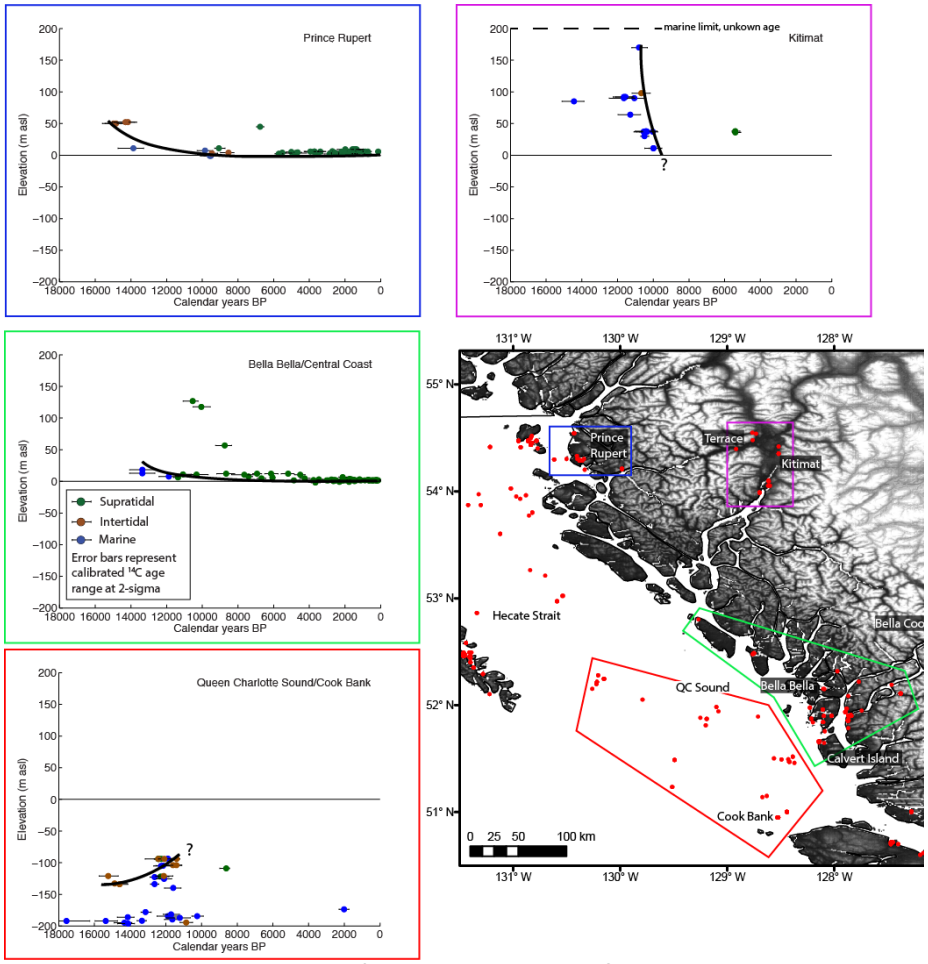

Figure 7. Relative sea level curve for the northern British Columbia sub-region, and part of the outer islands-north coast sub-region. Shown are southern Hecate Strait and Queen Charlotte (QC) Sound, and northern British Columbia mainland.

609

610 Evidence from archaeological sites and pond coring on the Dundas Island
611 archipelago, located at the eastern end of Dixon Entrance, ~40 km northwest of Prince
612 Rupert, suggests that RSL was about +12 m amsl by 14.1 to 13.8 ka BP and dropped
613 slowly to +9 m amsl by 12.2 to 12 ka BP and +5 m amsl by 8.3 to 8.2 ka BP (McLaren et
614 al., 2011). Since then, RSL has dropped slowly to the present level (Figure 8).

615 On Calvert Island on the outer central coast south of Bella Bella, Andrews and
616 Retherford (1978) described undated glaciomarine drift at +120 m amsl, which they
617 correlated to a similar deposit (+18 m amsl, 14.1 to 12.7 ka BP) on Denny Island, to the
618 north. The current authors were unable to locate any glaciomarine or glacial sediments
619 above about 32 m amsl at the Calvert Island location described by Andrews and
620 Retherford (1978). Archaeological sites at Namu, southeast of Bella Bella and northeast
621 of Calvert Island, provide evidence of sea level below +11 m amsl by 10.6 ka (Clague et
622 al., 1982a; Carlson and Bona, 1996). Based primarily on four submerged midden sites,
623 Andrews and Retherford (1978) argued that RSL dropped below present around 8.4 ka
624 BP on the central British Columbia coast, and remained below present until at least 1.9
625 to 1.6 ka BP. Cannon (2000), however, argued that as there are no gaps in
626 archaeological site ages at Namu to indicate a possible regression, RSL never dropped
627 below present and instead gradually and steadily declined over the course of the
628 Holocene (Figure 7). McLaren et al. (In review) provide substantial new evidence of
629 RSL history on the central coast. Based on more than 100 new radiocarbon dates from
630 Calvert Island and surrounding region, they argue that the region has experienced
631 relative stability over the past 15 ka and represents a sea level hinge.

3.4 Outer Islands-North Coast sub-region

During the Pleistocene, Haida Gwaii repeatedly supported mountain ice caps and local valley glaciers. There is limited evidence to suggest, however, that the Cordilleran Ice Sheet extended across Hecate Strait and coalesced with local ice sources on Haida Gwaii (Clague et al., 1982b; Clague, 1989b). Further north in southeast Alaska, glaciers probably reached only the inner continental shelf (Mann and Hamilton, 1995), but may have reached the outer shelf at major fjord mouths (Mann, 1986). Kaufman and Manley (2004) provided maps of Pleistocene maximum, Late Wisconsinan, and modern glacial extents for all of Alaska, but admit limited confidence in their maps for southeast Alaska.

During the LGM, which occurred at about 19 ka BP in northern coastal British Columbia and prior to 14 ka BP in the outer Alexander Archipelago (Heaton et al., 1996), parts of Haida Gwaii were ice-free (Warner et al., 1982; Heaton et al., 1996), possibly acting as glacial refugia. At that time, shorelines on eastern Graham Island in Haida Gwaii were probably no higher than present. The development of a crustal forebulge under Haida Gwaii resulted in RSL below -32 m amsl (17 to 15.5 ka BP) and -68 m amsl (11.2 to 10.6 ka BP) in adjacent northern Hecate Strait, -118 m amsl (11.1 to 10.2 ka BP) in central Hecate Strait, and -150 m amsl off of Moresby (15.0 to 13.5 ka BP) and Graham (14.9 to 13.0 ka BP) islands (Figure 8) (Barrie and Conway, 1999; Fedje and Josenhans, 2000; Barrie and Conway, 2002b; Hetherington et al., 2004). In Queen Charlotte Sound and the Cook Bank to the south, RSL was approximately -135 m amsl by 15.4 to 14.1 ka BP (Barrie and Conway, 2002b, a; Hetherington et al., 2003; Hetherington et al., 2004), rising to about -95 m amsl by 12.6 to 12.1 ka BP

(Figure 7) (Luternauer et al., 1989a; Luternauer et al., 1989b; Hetherington et al., 2003; Hetherington et al., 2004).

As the forebulge collapsed and migrated, a transgression occurred, reaching +5 m amsl by 10.5 to 9.6 ka BP (Fedje et al., 2005), to a high stand of about +15.5 m amsl by 9.1 to 8.2 ka BP on northern Graham Island (Figure 8) (Clague et al., 1982a; Wolfe et al., 2008). Between 9.1 to 8.2 and 5.6 to 4.8 ka BP, the sea regressed to below +8.5 m amsl (Clague, 1981, 1989b), causing foredune ridges on Naikoon Peninsula to prograde seaward (Wolfe et al., 2008). Relative sea level in northern Haida Gwaii continued to drop in the mid- to late Holocene (Clague et al., 1982a; Josenhans et al., 1997) with a possible abrupt regression from +8.5 to +4.5 m amsl between 6.5 to 4.8 ka BP and 2.9 to 2.5 ka BP, followed by a more gradual fall to +3 m amsl by 1.4 to 1.0 ka BP and +2 m amsl by approximately 550 years ago (Figure 8) (Wolfe et al., 2008).

On Moresby Island, archaeological data (Fedje et al., 2005) and isolation basin coring (Fedje, 1993; Fedje et al., 2005) indicate RSL remained above +14 m amsl between 11.1 and 6.9 ka BP, with a high stand below +19 m amsl being reached between 10.2 and 9.3 ka BP, after which it dropped slowly to the present datum (Fedje and Josenhans, 2000; Fedje et al., 2005). Although recent studies into the 2012 Haida Gwaii earthquake have documented a component of convergence along the predominantly strike-slip Queen Charlotte Fault (James et al., 2013; Lay et al., 2013; Szeliga, 2013), it is not known whether this has had a significant effect on RSL fluctuations since the LGM.

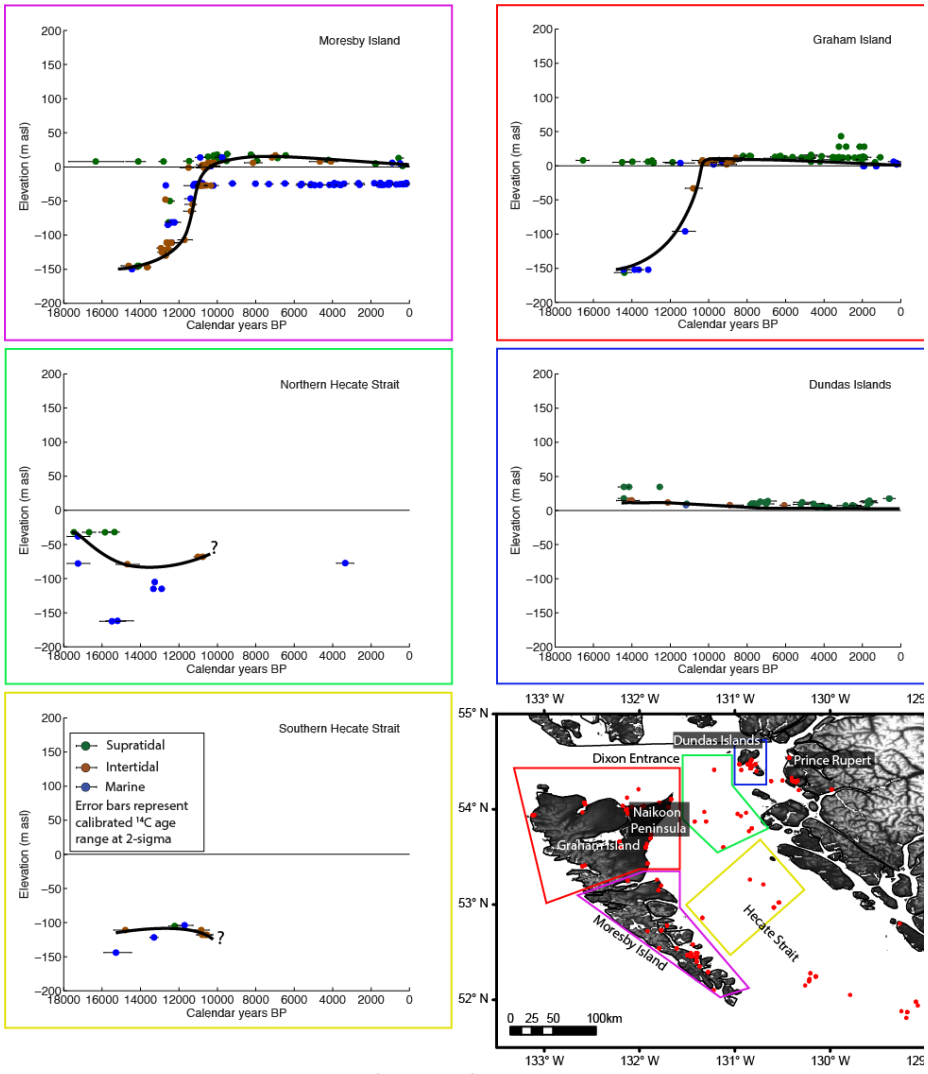

Figure 8. Relative sea-level curves for part of the outer islands-north coast sub-region, and part of the northern British Columbia sub-region. Shown are Haida Gwaii, Hecate Strait, and part of the northern British Columbia mainland.

To date, no age control for LGM glacier extents on the southwest islands of the Alexander Archipelago has been described. Records of late Pleistocene and Holocene RSL fluctuations on the outer coast region of the Alexander Archipelago however, closely resemble the pattern at Haida Gwaii to the south, although data below modern datum are relatively few. An undated wave-cut terrace exists at -165 m amsl off the west coasts of Prince of Wales and Baranof islands (Carlson, 2007). Freshwater lacustrine diatoms underlying marine shells (12.7 to 12.2 ka BP) and tephras (13.3 to 13.0 ka BP) in Sitka Sound on the west coast of Baranof Island suggest that RSL was below -122 m amsl prior to then (Figure 9) (Addison et al., 2010; Baichtal et al., 2012). Barron et al. (2009) described freshwater lacustrine diatoms (~14.2 to 12.8 ka BP based on age-depth modeling) underlying brackish diatoms (~12.8 to 11.1 ka BP, age-depth modeling) and marine shells (11.3 to 10.8 ka BP) in the Gulf of Esquibel off the west coast of Prince of Wales Island. Baichtal and Carlson (2010) later analyzed the bathymetry of the Gulf and identified a sill at -70 m amsl, which led them to argue that at the time the freshwater lake existed, RSL was below that elevation (Figure 9). The shell date provides a minimum age for the ensuing transgression in the Gulf of Esquibel, which rose above the present datum around 10.7 to 10.1 ka BP. A high stand of less than +16 m amsl at Heceta Island on the northern boundary of the Gulf of Esquibel was reached between 9.5 and 7.6 ka BP (Ackerman et al., 1985; Mobley, 1988; Baichtal and Carlson, 2010), while at Prince of Wales Island on the eastern boundary of the Gulf, RSL reached at least +14 m amsl by 9.8 to 9.1 ka BP. Following the high stands, the sea regressed, reaching below +14 m amsl on Heceta Island (Mobley, 1988) and

703 approximately +1 m amsl at Prince of Wales Island in the mid-Holocene (5.5 to 4.5 and
704 5.3 to 4.9 ka BP, respectively) (Figure 9).

705 ### 3.5 Southeast Alaska Mainland

706 Unlike in British Columbia, where studies of Holocene sea level have been
707 numerous and detailed (e.g. Andrews and Retherford, 1978; Clague, 1981; Clague et
708 al., 1982a; Clague, 1989c; Hutchinson, 1992; Josenhans et al., 1995; Josenhans et al.,
709 1997; James et al., 2009a), studies in much of southeast Alaska are more limited and
710 are largely exploratory in scope. Data pertaining to LGM glacial conditions in southeast
711 Alaska, in particular, are extremely sparse (D. Mann, *pers. comm.*, 2012).
712 Glaciers in southeast Alaska mainland began retreating around 16 to 14 ka BP
713 (Mann, 1986; Heaton and Grady, 1993, 2003; Mann and Streveler, 2008), which
714 corresponds roughly to the pattern of deglaciation in the Kodiak archipelago 1100 km to
715 the west (Mann and Peteet, 1994), but is several thousand years later than the
716 deglaciation of Dixon Entrance, east of Haida Gwaii (Barrie and Conway, 1999). By
717 comparison, glaciers in south-central Alaska and Haida Gwaii began retreating ~17 ka
718 BP and ~19 ka BP, respectively. Irrespective of the LGM limits, multiple still-stands and
719 re-advances occurred in southeast Alaska during recession from the LGM (Barclay et
720 al., 2009).
721

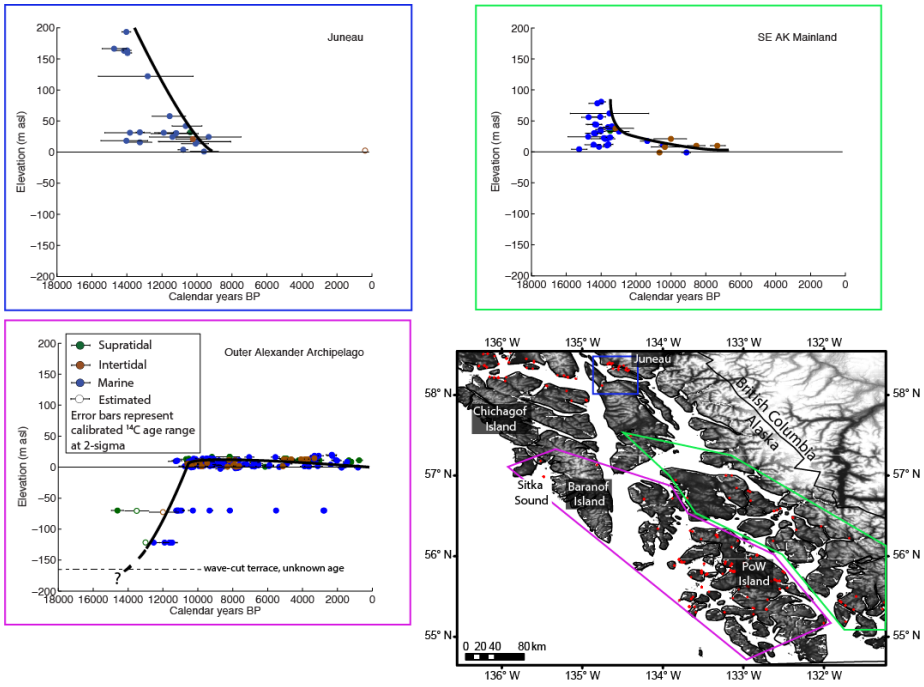

Figure 9. Relative sea-level curves for part of the outer islands-north coast sub-region, and part of the southeast Alaska mainland sub-region. Shown are the islands of the Alexander Archipelago, including Prince of Wales (PoW) Island.

Post-glacial RSL fluctuations in southeast Alaska are somewhat better constrained by field data than LGM glacial limits. A widespread marine transgression reached to between +50 and +230 m amsl in Gastineau Channel near Juneau prior to ~15 ka BP (Figure 9) (Mann, 1986; Mann and Hamilton, 1995), above +51 m amsl on the Chilkat Peninsula in Icy Strait by 14.2 to 13.7 ka BP (Figure 10) (Mann and Streveler, 2008), above +62 m amsl near Petersburg on Mitkof Island by 15.8 to 11.3 ka BP (Figure 9), and +70 m amsl on Chichagof Island by 13.3 to 12.8 ka BP (Mann, 1986). In Adams Inlet in upper Glacier Bay however, McKenzie and Goldthwaite (1971) argued that RSL

735 was still about +90 m amsl by 13.1 to 12.6 and +60 m amsl by 12.7 to 11.3 ka BP
736 (Figure 10), while at Juneau, it was still above +193 m amsl by 14.3 to 13.8 ka BP
737 (Figure 9) (Baichtal et al., 2012).
738

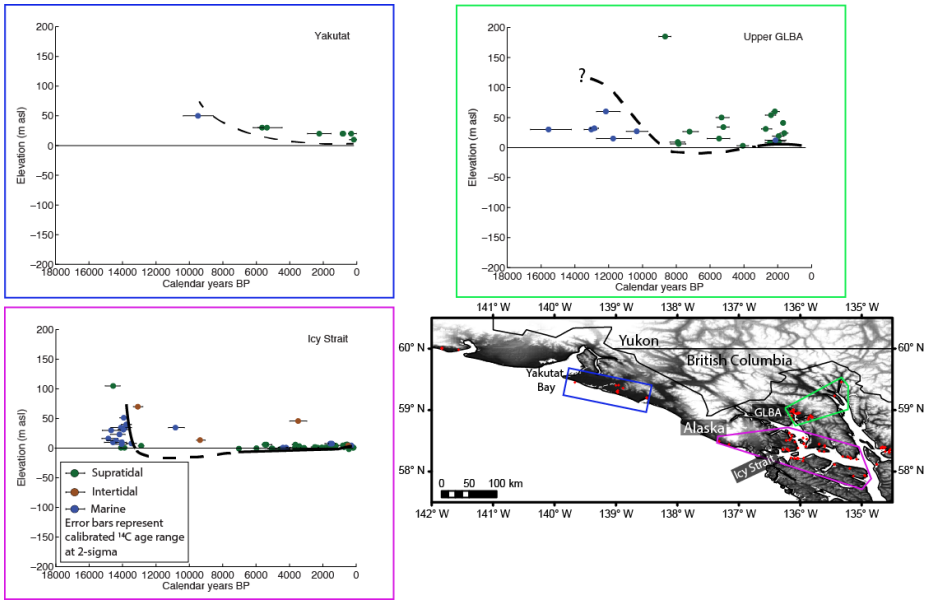

739
740 Figure 10. Relative sea-level curves for part of the southeast Alaska mainland sub-
741 region. Shown are Icy Strait, Glacier Bay (GLBA), and the Yakutat Bay region.
742

743 Following this, RSL in Icy Strait dropped very rapidly to below present datum soon
744 after 14.2 to 14.0 ka BP (Figure 10) (Mann and Streveler, 2008). Little stratigraphy or
745 landforms to define RSL between about 13 and 7 ka BP have been identified in Icy
746 Strait, leading Mann and Streveler (2008) to argue that the sea must have been a few
747 meters below present for that time. In eastern Icy Strait, on the Chilkat Peninsula and
748 northeast Chichagof Island, there is limited evidence that RSL may have been above

749 present during this time. In the mid-Holocene, RSL in Icy Strait began a fluctuating rise
750 likely in response to isostatic depression and rebound from Glacier Bay, but stayed
751 below present datum for most of the late Holocene (Figure 10).
752 During the LIA, parts of the southeast Alaska mainland sub-region were
753 isostatically depressed by massive ice loads (Larsen et al., 2005) that led to an RSL
754 high stand of about +2 m amsl in Icy Strait (Figure 10) (Mann and Streveler, 2008). This
755 is similar, though at the low end of the range of +3 to +5.7 m amsl provided by Larsen et
756 al. (2005) for Glacier Bay, which experienced thicker ice. Near Juneau, Motyka (2003)
757 documented a LIA sea-level transgression to +3.2 m amsl above current sea level that
758 stabilized about 450 years ago. Using dendrochronology and the geomorphology of a
759 sea-cliff eroded into late-Pleistocene glaciomarine sediments, Motyka (2003)
760 demonstrated that Sitka spruce colonized newly emergent coastal terrain as it was
761 uplifted following the transgression. He argues that the land began emerging between
762 AD 1770 and 1790, coincident with regional glacial retreat, and has uplifted ~3.2 m
763 since then.
764 Larsen et al. (2005) found that uplift rates associated with current ice thinning
765 explained about 40% of observed uplift near the Yakutat Icefield (32 mm a^{-1}) and only
766 15% in Glacier Bay (30 mm a^{-1}). They expected less than a 5 mm a^{-1} tectonic
767 contribution to the observed uplift, due to the strike-slip nature of the Fairweather Fault
768 in their study area. Instead, their geodynamic modeling suggested that post-LIA
769 isostatic rebound is responsible for the bulk of the observed uplift. Further, they argued
770 that the region has regained only about one-half of its LIA subsidence and that another
771 6 to 8 m of uplift will occur in Glacier Bay over the next 700 to 800 years, as a result of

772 ice already lost. Importantly, these results demonstrate that isostatic depression can be
773 an extremely localized phenomenon.

774 ### 3.5 South-Central Alaska

775 At the LGM, glaciers covered nearly all of the Kenai Peninsula and filled Cook
776 Inlet. The maximum extent of glaciers onto the continental shelf in the Gulf of Alaska is
777 unresolved (c.f. Péwé, 1975), but several authors (e.g. Mann and Hamilton, 1995;
778 Molnia and Post, 1995) argued that it flowed to the outer edge of the shelf. Reger and
779 Pinney (1995) estimated that ice thickness around Kenai was around 315 to 335 m
780 between 25 and 21.4 ka BP, resulting in about 100 m of isostatic depression. In
781 contrast, they argued that the area around Homer, at the south end of Kenai Peninsula,
782 was not isostatically depressed by Late Wisconsin ice nearly as much. At Anchorage to
783 the north, Reger and Pinney (1995) estimated ice thickness was a minimum of 285 m,
784 resulting in about 85 m of isostatic depression and RSL about +36 m amsl above
785 present prior to approximately 16.3 ka BP.
786 Maximum glacier extent in south-central Alaska was out of phase with that in
787 southern British Columbia, with northern glaciers reaching their outer limits between
788 27.6 and 19.1 ka BP, compared to 18 to 17 ka BP further south (Mann and Hamilton,
789 1995). Deglaciation was similarly time-transgressive, with glaciers retreating from the
790 continental shelf of south-central Alaska before 19 ka BP and those in southwest British
791 Columbia beginning retreat about 2 to 3 ka later (Mann and Hamilton, 1995; Shennan,
792 2009).
793 Data to constrain RSL during the late Pleistocene and early Holocene in south-
794 central Alaska are scant, but a number of sites record a regression during much of the

Holocene. As glaciers in Cook Inlet began to break up, RSL was at least +10 m amsl at 19.1 to 18.7 ka BP (Figure 11) (Mann and Hamilton, 1995; Reger and Pinney, 1995). Schmoll et al. (1972) suggested that shell-bearing clays near Anchorage, between +10 and +14 m amsl and dating from 16.8 to 14.6 ka BP were formed during a marine transgression during an early post-glacial phase of eustatic sea-level rise, although Mann and Hamilton (1995) argue that glacio-isostatic depression resulted in the high stand. The shell-bearing sediments described by Schmoll et al. (1972) extend to an elevation of +36 m amsl, leading Reger and Pinney (1995) to argue that RSL was at least that high between 16.8 to 14.6 ka BP. Although the elevation of the high stand is unknown, peat at +24 m amsl suggests that RSL in Cook Inlet was below that elevation by 16.2 to 14.2 ka BP (Rubin and Alexander, 1958). No data currently exist for the Cook Inlet region between 11.1 and 6.7 ka BP, but peats from 6.7 to 6.3 ka BP suggest RSL was below +2 m amsl by then. By 3.9 to 3.6 ka BP at Girdwood in upper Cook Inlet, the sea began to transgress from below -2 m amsl and likely did not rise above present datum. An antler bone from -2.5 m amsl suggests that RSL was still below this level by 3 to 2.7 ka BP (Figure 11).

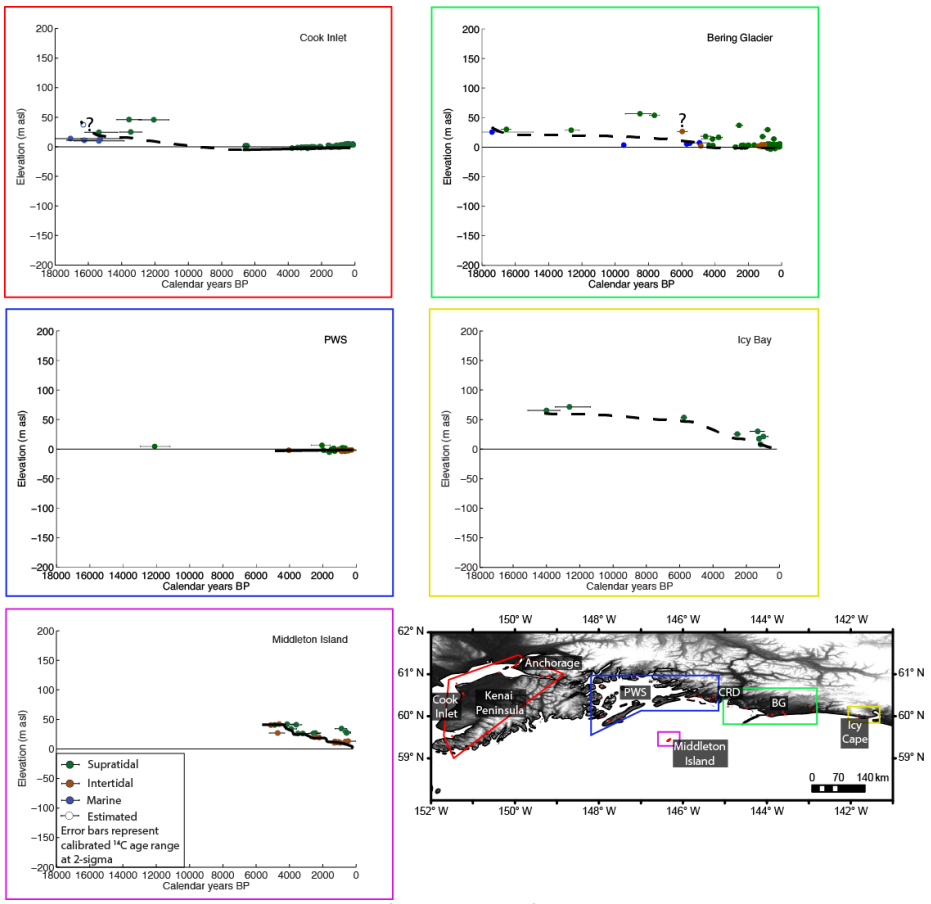

Figure 11. Relative sea-level curves for the south-Central Alaska sub-region, including Prince William Sound (PWS), the Copper River delta (CRD), Bering Glacier (BG), and Cook Inlet. A sample of *Modiolus* shell (26 masl, 6.3-5.7 ka BP) collected by Sirkin and Tuthill (1969) at Katalla, near Bering Glacier, is anomalous according to the original authors.

Comment [DS2]: Note to editor and reviewers that Figure 11 has been updated with additional data.

To the east, between Prince William Sound and Bering Glacier, a peat at +30 m amsl constrains RSL around 16.8 to 16.3 ka BP (Peteet, 2007), while a peat on a marine terrace at +56 m amsl at Katalla, midway between the Copper River delta and Bering Glacier, suggests RSL rose prior to 9.4 to 7.8 ka BP (Figure 11) (Plafker, 1969).

It is conceivable, however, that the peat is significantly younger than the actual terrace age, and no early-Holocene transgression to +56 m amsl occurred, but rather that the terrace was formed prior to formation of the +30 m amsl terrace. RSL then rapidly fell to +2 m amsl by 4.8 to 4.4 ka BP and to -2 m amsl by 4.8 to 3.3 ka BP (Plafker, 1969; Molnia and Post, 1995; Shennan, 2009). Unfortunately, the broad depth range (~22 m) of the bivalves used by Shennan (2009) from the early- to mid-Holocene preclude precise estimation of RSL positions. By 1.8 to 1.4 ka BP, RSL was below -5.2 m amsl before rising to the present datum (Figure 11).

At Icy Cape, marine terraces record regression from between +66 and +72 m amsl between 15.1 and 11.4 ka BP, to +54 m amsl around 5.9 to 5.6 ka BP, +26 m amsl at 2.7 to 2.4 ka BP, and +18 m amsl by 1.3 to 1.1 ka BP (Figure 11) (Plafker et al., 1981). At Middleton Island, located near the edge of the continental shelf south of Prince William Sound, six marine terraces record regression from +41 m amsl (~5.3 to 4.5 ka BP), to +34 m amsl (4.5 to 3.8 ka BP), to +26 m amsl (3.6 to 3.0 ka BP), to +20 m amsl (2.7 to 2.2 ka BP), to +13 m amsl (1.5 to 1.0 ka BP), and to +6.4 m amsl (AD 1964) (Figure 11) (Plafker and Rubin, 1978).

4.0 Discussion

Strong spatial gradients in RSL exist along the shores of the northeastern Pacific Ocean due to the complex and often competing influences of glacial ice loading and retreat, crustal rheology, and tectonic setting (Mann and Streveler, 2008). Regions of dissimilar RSL history are described as being separated by “hinge zones” where relatively little change occurs (Figure 12) (e.g. McLaren et al., 2011; McLaren et al., In

review). It is important to note however, that such a hinge was unlikely static in space or time.

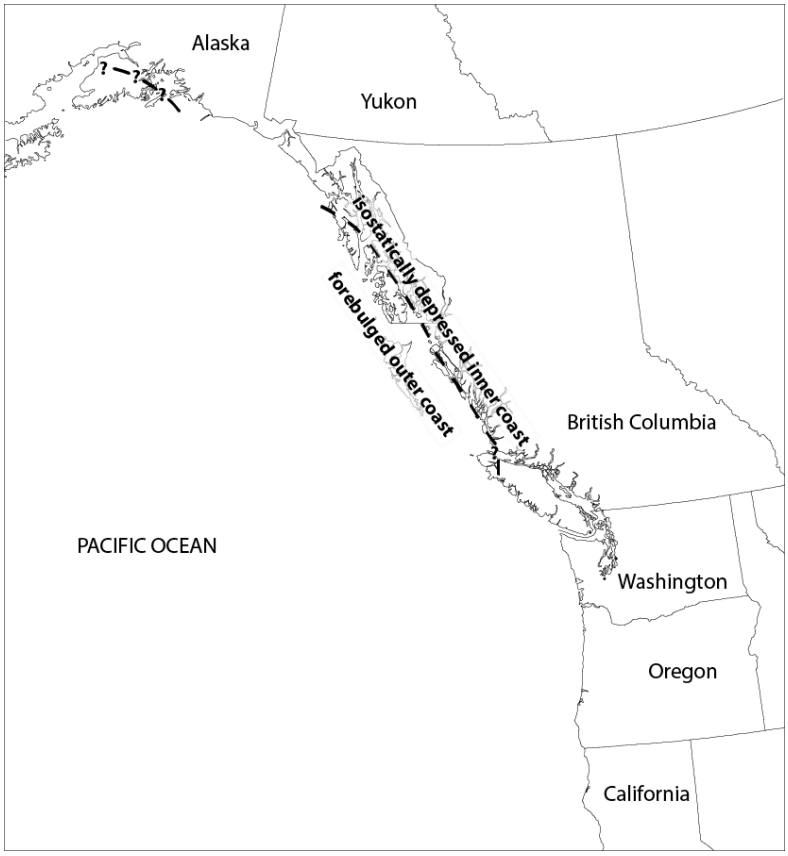

Figure 12. Map of the Pacific coast of North America showing hypothesized sea level hinge between areas that were isostatically depressed and areas that were uplifted as a result of a forebulge.

The northeastern Pacific region can thus be subdivided into broad zones, based on the main factor(s) governing RSL response. Such zones, as discussed here, include

areas governed predominantly by: (1) the distance to large ice masses and associated isostatic movements; or (2) crustal movements not related to ice masses.

4.1 Regions controlled by isostasy

In parts of the study area, magnitudes of RSL adjustments are far too large to be explained by anything other than glacio-isostasy and eustasy. These include northern Cascadia, northern British Columbia, and southeast Alaska.

4.1.1 Northern Cascadia

Rapid crustal deformation due to advance and retreat of continental glaciers was the main driver of RSL changes on the British Columbia coast during the late Quaternary (e.g. Clague et al., 1982a). This explanation also holds true for the Puget lowlands of Washington, which experienced more than 100 m of sea-level rise due to isostatic depression at the end of the Fraser Glaciation. Similarities exist between the sea level curves within northern Cascadia, but with significant differences in timing and magnitudes. Most regions experienced early post-glacial marine high stands due to significant isostatic depression, followed by a rapid regression as the land rebounded (e.g. Lower Mainland, Figure 5). In some areas, RSL steadily declined to modern-day levels, while in others RSL fell below present during part of the Holocene. In general, areas that were deglaciated first were inundated first; the Puget lowlands saw marine high stands about 700 years before Vancouver, British Columbia, to the north, which in turn was flooded 400 years prior to parts of the Fraser Valley to the east.

Sea level regressions in northern Cascadia were equally time-transgressive. On western Vancouver Island, the marine low stand occurred nearly 2,000 years before the low stand on eastern Vancouver Island (Figure 6) (James et al., 2009a), and 4,800 years before the low stand in the Lower Mainland (Clague et al., 1982a; James et al., 2002).

Subsequent RSL rises in southern British Columbia also differ in their rates and positions relative to present shorelines. On western Vancouver Island, RSL rose to a few meters above present in about five thousand years during the first half of the Holocene (Friele and Hutchinson, 1993; Dallimore et al., 2008), and has been dropping slowly since (Figure 6). Following a low stand in the central Strait of Georgia in the early Holocene, RSL rose to above present within two to three thousand years, and has been dropping slowly since (Hutchinson et al., 2004). At Victoria on southeast Vancouver Island, and in Vancouver area on the mainland, however, RSL rose gradually to present levels but did not submerge present shorelines (Clague et al., 1982a; James et al., 2009a). The differences in timing and magnitude of RSL changes in southern British Columbia are not due to a forebulge, as in Haida Gwaii, but rather result from relative thickness of, and distance to, former ice masses and local tectonics. The lowstand of -46 m amsl identified on western Vancouver Island however, may be due to a forebulge effect, and requires further investigation (Friele and Hutchinson, 1993). The nearly unvarying RSL histories for the Broughton Archiplego/Queen Charlotte Strait and northern Vancouver Island regions (Figure 6) suggest that this region may represent the southern extent of the hinge zone (Figure 12). This statement however, should be

898 treated with some caution due to the small number of pre-mid-Holocene data points
899 defining the RSL curve.
900 There is no question that neotectonic deformation has also influenced RSL over
901 the late Quaternary in northern Cascadia (Leonard et al., 2010). Along the outer coast
902 of Washington, earthquakes and resulting coseismic subsidence on the range of 0.5 to
903 2.0 m resulted in burial of well-vegetated lowlands by intertidal muds at least six times in
904 the past 7 ka (Atwater, 1987). Although the onset of such events is geologically rapid,
905 the magnitudes of RSL change are generally minor compared to the scales of RSL
906 change caused by isostatic effects.

907 ***4.1.2 Northern British Columbia***

908 As in northern Cascadia, isostatic crustal displacements have governed late
909 Quaternary RSL changes on the northern British Columbia coast (e.g. Riddihough,
910 1982; Barrie and Conway, 2012). Many authors have commented on the dichotomy
911 between post-glacial RSL on Haida Gwaii (Figure 8) and fjord heads on mainland British
912 Columbia (e.g. Kitimat, Figure 7) (e.g. Clague et al., 1982a; Clague, 1989a; Luternauer
913 et al., 1989a; Barrie and Conway, 2002b; Hetherington et al., 2003). The fjord heads
914 experienced much higher marine high stands because the crust was severely
915 isostatically depressed and inundated prior to significant rebound. On Haida Gwaii, far
916 from the centre of the Cordilleran Ice Sheet, a crustal forebulge raised the land relative
917 to the sea, causing RSL to fall. Recently, McLaren et al. (2011) argued that the Dundas
918 Island archipelago (Figure 8) represents the hinge point separating the isostatically
919 depressed mainland and the forebulged outer coast, while McLaren et al. (In review)
920 extended the hinge south through the British Columbia central coast (Figure 12).

Ongoing RSL changes in northern British Columbia are almost certainly tectonic in origin (Mazzotti et al., 2008), although their magnitudes are insignificant when compared to fluctuations over the late Quaternary (Riddihough, 1982).

4.1.3 Outer Islands-North Coast

The RSL history of the outer islands-north coast region (Figures 8, 9) diverges sharply from that experienced closer to the center of the ice sheet on the mainland (e.g. Figure 7), resulting in a northward continuation of the hinge zone described for the Dundas Islands (McLaren et al., 2011), the British Columbia central coast (McLaren et al., In review), and the Broughton Archiplego/Queen Charlotte Strait and northern Vancouver Island region described above (section 4.1.1, Figure 12). On the now-drowned Hecate plain, RSL fell for the first two millennia after deglaciation and then rose during the next several thousand years due to the passage of the crustal forebulge (Figure 8). A high stand above the modern datum was then reached during the early Holocene.

Prince of Wales Island and Baranof Island, as well as many smaller islands in the outer Alexander Archipelago of southeast Alaska, were submerged under 165 m of water at the same time as areas to the east such as Juneau and the southeast Alaska mainland were 200 m and 100 m above RSL. The sea level curve for the outer Alexander Archipelago (Figure 9) is similar to that for Haida Gwaii (Figure 8) both in magnitude and timing. These patterns led Carrara et al. (2007) to argue that a crustal forebulge developed on the western margin of the Alexander Archipelago.

4.1.3 Southeast Alaska Mainland

The lack of evidence for substantial late-Pleistocene emergence in Icy Strait (Figure 10) lead Mann and Streveler (2008) to suggest that a migrating forebulge was not involved in deglacial geodynamics of the area. Mann and Streveler (2008) contend that the RSL history in Icy Strait instead resembles that of southern Vancouver Island, where land emergence culminated in the early Holocene with shorelines below present sea levels (c.f. Figure 12). In the early Holocene, residual isostatic rebound on both southern Vancouver Island and in Icy Strait was roughly balanced by eustatic sea-level rise. In Icy Strait, however, the similarity between the curves was disrupted by repeated isostatic adjustments to local glacier fluctuations since about 5 ka BP (Mann and Streveler, 2008).

In the late Holocene, RSL in much of southeast Alaska was mainly controlled by isostatic rebound, whereas in southern British Columbia, isostatic rebound was probably complete much earlier. Several investigators have argued that some or most of the current regional uplift in southeast Alaska, is tectonic in origin (e.g. Horner, 1983; Savage and Plafker, 1991). Recent studies, however, have demonstrated that uplift in southeast Alaska is related primarily to post-LIA and contemporary glacial unloading (e.g. Hicks and Shofnos, 1965; Motyka, 2003; Motyka and Echelmeyer, 2003; Larsen et al., 2005; Doser and Rodriguez, 2011; Sato et al., 2011).

While a hinge zone separating the isostatically depressed southeast Alaska mainland region from the forebulged outer coast has been identified (Figure 12), differences in RSL also exist along a north-south transect within the southeast Alaska mainland region. In the late Pleistocene, when RSL was several meters below modern

965 levels in Icy Strait (Mann and Streveler, 2008), it was +90 m above present datum in
966 Adams Inlet in upper Glacier Bay (McKenzie and Goldthwait, 1971). The discrepancy
967 between the Adams Inlet and Icy Strait records is due to differential isostatic response,
968 as Adams Inlet was much closer to large ice masses during the LGM. In this way,
969 similar processes as in northern Cascadia appear to govern RSL changes in parts of
970 southeast Alaska.

971 ## 4.2 Regions controlled by neotectonics

972 Most of the evidence for RSL fluctuations in southern Cascadia and south-central
973 Alaska comes from studies of vertical land displacements resulting from subduction-
974 zone earthquakes. Similar sequences of peats and muds in both sub-regions have been
975 interpreted as representing sudden co-seismic submergence, followed by slower
976 interseismic uplift and RSL regression. Post-glacial marine high stands in these regions
977 have not been well described.

978 ### *4.2.1 Southern Cascadia*

979 Intercalated sequences of organic and inorganic sediments in Washington and
980 Oregon (Atwater, 1987; Atwater and Yamaguchi, 1991) reflect a repetitive sequence of
981 crustal movements that Long and Shennan (1994) termed the “earthquake deformation
982 cycle”. In general, these couplets are too wide-spread (>100 km), too thick (>1 m), and
983 have been deposited too rapidly (<10 yr) to be attributed to any process except coastal
984 subsidence during an earthquake (Nelson and Kashima, 1993). Several authors have
985 described great earthquakes in southern Cascadia with recurrence intervals between a
986 few hundred and 1000 years (Witter et al., 2003; Nelson et al., 2006). The magnitudes

of RSL change resulting from repeated coseismic deformation is not large. Litho- and biostratigraphic data from Johns River, Washington, and Netarts Bay, Oregon, for example, show evidence for repeated episodes of coseismic subsidence of up to 1.0 ± 0.5 m over the past 4 ka (Long and Shennan, 1998), while peat-mud couplets from Alsea Bay, Oregon, show coseismic subsidence of <0.5 m four times over the past 2 ka (Nelson et al., 2008). Although pre-Holocene data are sparse in southern Cascadia, eustatic changes almost certainly would have governed RSL dynamics at this time.

4.2.2 South-Central Alaska

Similar estuarine stratigraphy to that in southern Cascadia has been found in south-central Alaska (e.g. Hamilton and Shennan, 2005a), suggesting that the role of non-isostatic tectonic crustal deformation in RSL dynamics is important in both regions. Estuarine mud buried lowland soils in south-central Alaska following the 1964 Alaska Earthquake (Ovenshine et al., 1976) and an earlier earthquake at approximately 1.7 to 1.4 ka BP (Hamilton and Shennan, 2005a). This earthquake caused 2.4 m of coseismic subsidence near Anchorage and resulted in deposition of as much as 1.5 m of fine-grained intertidal sediment (Ovenshine et al., 1976).

Marine terraces near Icy Cape were interpreted by Plafker et al. (1981) to indicate that most crustal deformation in the region was caused by neotectonics, with minimal uplift due to isostatic rebound (Figure 11). Their uplift rate for the Icy Cape region averaged 10.5 mm a^{-1} since the mid-Holocene, which is remarkably similar to that at Middleton Island (~10 mm a^{-1}) where marine terraces record emergence from the sea during six major episodes of coseismic uplift (Figure 11) (Plafker and Rubin, 1978).

Such uplifted terraces are believed to document a series of upward coseismic pulses separated by intervals of stability or even gradual submergence (Plafker, 1990).

At Girdwood in Cook Inlet on the other hand, Plafker (1969) noted subsidence rates of about -2-3 mm a^{-1} between 3.4 to 2.5 and 1.2 to 1.0 ka BP. In upper Cook Inlet, all of the recorded great earthquakes in the past 3 ka BP have been accompanied by pre-seismic land subsidence (Shennan and Hamilton, 2006). This submergence contrasts with the emergence and RSL fall through the preceding inter-seismic period of each earthquake cycle (Figure 2). For example, during the AD 1964 Alaska earthquake, tidal marshes and wetlands in upper Cook Inlet experienced up to 2 m of subsidence (Shennan and Hamilton, 2006). Freymueller et al. (2008) described the pattern of vertical velocities in south-central Alaska as agreeing with the classic interseismic strain model, with subsidence found near the coast and offshore, and uplift found inland. Their measurements on Kenai Peninsula for example, indicate >1.1 m of cumulative uplift following the AD 1964 Alaska earthquake. Great earthquakes in south-central Alaska tend to have a recurrence interval of about 1000 years (Mann and Hamilton, 1995).

The modern tectonics of coastal south-central Alaska are complicated with respect to their influence on RSL. Some areas have experienced coseismic uplift (e.g., in response to the 1964 AD earthquake) but long-term submergence (i.e., tectonic subsidence combined with eustatic sea-level rise), while other regions have experienced coseismic and long-term emergence or coseismic subsidence. For example, in Prince William Sound and the Copper River valley, Plafker (1990) documented pre-1964 submergence over at least 800 years at rates ranging from about -5 to 8 mm a^{-1}, averaging about -7 mm a^{-1}. Tide gauge data showed uplift rates of +2.7

+/- 1.5 mm a^{-1} at Seward and +4.8 +/- 1.6 mm a^{-1} at Kodiak, Alaska, in the decades preceding the 1964 earthquake (Savage and Plafker, 1991). More recently, Cohen and Freymueller (2004) analyzed post-seismic deformation across the area affected by the 1964 earthquake and found over 1 m of cumulative uplift, but with considerable temporal and spatial variability. Using 15 years of GPS measurements, Freymueller et al. (2008, see their Plate 1) mapped contemporary (AD 1992 to 2007) deformation patterns from south-central Alaska, showing that much of Cook Inlet on the west side of the Kenai Peninsula is undergoing post-seismic uplift, while Prince William Sound on the east side of the Kenai Peninsula is subsiding. Plafker (1969) noted that in south-central Alaska, areas of net Holocene coastal emergence or submergence broadly correspond with areas where significant amounts of uplift or subsidence occurred during the 1964 Alaska earthquake. From this, Plafker (1969) deduced that differential RSL changes and resulting displacements in south-central Alaska must result largely from tectonic movements.

Although RSL changes in south-central Alaska may be governed predominantly by neotectonics, Hamilton and Shennan (2005a, b) suggested that relatively small RSL oscillations could also reflect either local sediment consolidation (e.g. 0.9 m associated with the 1964 earthquake) or longer-term isostatic adjustments. Ice thickness and resulting isostatic depression were much less in south-central Alaska than mainland British Columbia (c.f. Reger and Pinney, 1995), which partly explains why post-glacial marine high stands are considerably lower in south-central Alaska than in much of coastal British Columbia.

4.3 Research gaps and future directions

Significant work by Quaternary geologists, geomorphologists, seismologists, and archaeologists has provided valuable insight into the post-glacial sea-level history along much of the northwestern coast of North America. Despite decades of effort, however, appreciable spatial and temporal gaps remain in our understanding. In particular, knowledge of early post-glacial RSL trends and landscape responses in south-central Alaska and along the central British Columbia coast is limited. The data shown in Figure 11 for Prince William Sound and Cook Inlet in particular, indicate that a hinge zone may be present in south-central Alaska (Figure 12). However, no data exist to support the existence of a forebulge offshore. More work is required to validiate or refute this possibility. Knowledge of RSL dynamics in the southern Alexander Archipelago in Alaska in the early post-glacial period, and further south in the southern Puget Sound region is also limited. Furthermore, the relative roles of tectonic and other forcing mechanisms on RSL in southern Cascadia are poorly known.

Research to address these gaps is vitally important for: (i) reconstructing post-glacial landscape evolution along the northwestern coast of North America over the late Quaternary; (ii) understanding the peopling of North America; (iii) understanding the regional biogeography and speciation of coastal flora and fauna; (iv) improving knowledge and mitigation of co- and post-seismic coastal landscape hazards; and (v) modeling the implications of ongoing and future sea-level changes. McLaren et al. (In review) describe a sea level hinge on the central coast of British Columbia and provide critical new data to fill some of these gaps. Their analysis reveals that the same

shoreline has been inhabited continuously for more than 10,000 years as a direct result of the stability of RSL.

Recent technological developments that improve our temporal (e.g. optical dating) and spatial (e.g. LiDAR mapping) resolution have facilitated improved Quaternary landscape reconstructions in coastal sites around the world (e.g., Clague et al., 1982b; Litchfield and Lian, 2004; Wolfe et al., 2008; Rink and López, 2010; Bowles and Cowgill, 2012; Mauz et al., 2013). LiDAR techniques are especially useful in areas such as the northeast Pacific coast, where heavy vegetation obscures raised shoreline features. Optical dating, on the other hand, is valuable for dating of sedimentary landforms not suitable for radiometric methods, such as relict coastal dunes and beaches.

5.0 Summary

Relative sea levels are governed by a number of geophysical factors, including glacial isostasy, neotectonics, eustasy, and steric effects. We synthesize ~2,200 radiocarbon ages pertaining to post-glacial relative sea levels in Pacific North America, from northern California to south-central Alaska and provide rationale for dividing the coast into self-similar regions where RSL is governed mainly by one mechanism or another.

The late Quaternary sea level history of southern Cascadia is characterized by a probable low stand of around -120 m due to eustatic lowering at the end of the last glaciation (Clark and Mitrovica, 2011), followed by a marine transgression to slightly below present (Figure 4). In the latter half of the Holocene, relative sea level in southern Cascadia has risen to the present datum. Earthquakes and co-seismic crustal

displacements have caused repeated fluctuations in RSL in southern Cascadia throughout the Holocene.

The late Quaternary sea level histories of northern Cascadia, northern British Columbia, and the southeast Alaska mainland are governed primarily by isostatic depression and rebound in concert with eustasy. The Cordilleran Ice Sheet depressed the land over which it formed, which resulted in marine high stands up to +200 m above present in southwest British Columbia. Areas that were farther from the thicker parts of the ice sheet were depressed less and, hence, RSL high stands were lower. As the land rebounded in early postglacial time, RSL dropped rapidly, reaching low stands of -11 m near Vancouver, -30 m near Victoria, and -46 m on western Vancouver Island. Since these low stands, RSL has transgressed to present levels and, in some areas, has reached a Holocene high stand prior to regressing to present levels.

The late Quaternary RSL history of the outer islands-north coast region is also dominated by isostatic effects, but in a more complex fashion than in northern Cascadia. An isostatic forebulge under Haida Gwaii and the outer Alexander Archipelago resulted in early post-glacial RSL around -150 m below present. As the forebulge migrated as it collapsed, the ocean transgressed the land and reached a Holocene high stand up to +18 m above present before regressing to the present level.

The late Quaternary sea level history of southeast Alaska mainland is dominated by isostatic effects, with late Pleistocene high stands up to +200 m near Juneau, and rapid transgression as the land rebounded. The southeast Alaska mainland is the only region in this study in which late neoglacial isostatic effects during the Little Ice Age had a substantive effect on RSL fluctuations.

In south-central Alaska, late Quaternary RSL history is governed primarily by neotectonics, even though the region was glaciated during the LGM. Marine high stands are relatively low, ranging from above +36 m amsl near Anchorage to +56 m amsl near Bering Glacier. More work is required to determine whether the region represents a hinge zone and if so, whether a crustal forebulge developed offshore.

Geographic and temporal data gaps remain in our understanding of post-glacial RSL dynamics in northwestern North America. Recent technological advancements that facilitate higher resolution mapping of paleo-shorelines in hitherto unexplored locations, coupled with modern absolute dating methods (e.g., OSL) that are not reliant on carbonaceous material for dating, will allowing researchers to better identify and develop detailed chronologies for RSL dynamics and related landscape evolution.

6.0 Acknowledgements

This work was supported by grants from the Tula Foundation and NSERC to IJW and OBL, support from the Tula Foundation to DF, postdoctoral fellowships from the Tula Foundation and MITACS-Elevate to DHS, postdoctoral fellowships from the Tula Foundation to CMN and DM, and graduate fellowships from the Tula Foundation and NSERC to JBRE. Many people helped with the compilation of the database presented here (in some cases retrieving and interpreting decades-old field notes), including (in alphabetical order): Robert Ackerman, James Baichtal, Natasha Barlow, Vaughn Barrie, John Clague, Ian Hutchinson, Thomas James, Dan Mann, Roman Motyka, Dorothy Peteet, Peter Ruggiero, Norm Shippee, and Ian Shennan. Further, two anonymous reviewers and Editor-in-Chief Colin Murray-Wallace made excellent suggestions that greatly improved the paper.

7.0 References

Ackerman, R.E., Reid, K.C., Gallison, J.D., Roe, M.E., 1985. Archaeology of Heceta Island: a survey of 16 timber harvest units in the Tongass National Forest, southeastern Alaska. Report No. 3, Center for Northwest Anthropology, Washington State University, Pullman.

Addison, J.A., Beget, J.E., Ager, T.A., Finney, B.P., 2010. Marine tephrochronology of the Mt. Edgecumbe Volcanic Field, Southeast Alaska, USA. Quat. Res. 73, 277-292.

Allan, J.C., Komar, P.D., Priest, G.R., 2003. Shoreline variability on the high-energy Oregon coast and its usefulness in erosion-hazard assessments. J. Coastal Res. 38, 83-105.

Allison, M.A., 1998. Historical changes in the Ganges-Brahmaputra Delta front. J. Coastal Res. 14, 1269-1275.

Andrews, J.T., Retherford, R.M., 1978. A reconnaissance survey of late Quaternary sea levels, Bella Bella/Bella Coola region, central British Columbia coast. Can. J. Earth Sci. 15, 341-350.

Antonov, J.I., 2005. Thermosteric sea level rise, 1955–2003. Geophysical Research Letters 32.

Armstrong, J.E., 1981. Post-Vashon Wisconsin glaciation, Fraser Lowland, British Columbia. Bulletin 322, Geological Survey of Canada, Ottawa.

Atwater, B.F., 1987. Evidence for Great Holocene earthquakes along the outer coast of Washington State. Science 236, 942-944.

Atwater, B.F., Yamaguchi, D.K., 1991. Sudden, probably coseismic submergence of Holocene trees and grass in coastal Washington State. Geology 19, 706-709.

Baichtal, J.F., Carlson, R.J., 2010. Development of a model to predict the location of early Holocene habitation sites along the western coast of Prince of Wales Island and the outer islands, Southeast Alaska. Current Research in the Pleistocene 27, 64-67.

Baichtal, J.F., Carlson, R.J., Smith, J., Landwehr, D., 2012. The paleogeography, glacially induced crustal adjustments, and early Holocene climates from analysis of shell-bearing raised marine deposits. Alaska Temperate Coastal Rainforest Conference, Juneau.

Barclay, D.J., Wiles, G.C., Calkin, P.E., 2009. Holocene glacier fluctuations in Alaska. Quat. Sci. Rev. 28, 2034-2048.

1178 Bard, E., Hamelin, B., Delanghe-Sabatier, D., 2010. Deglacial meltwater pulse 1B and
1179 Younger Dryas sea levels revisited with boreholes at Tahiti. Science 327, 1235-1237.

1180 Barlow, N.L.M., Shennan, I., Long, A.J., 2012. Relative sea-level response to Little Ice
1181 Age ice mass change in south central Alaska: Reconciling model predictions and
1182 geological evidence. Earth Plan. Sci. Lett. 315-316, 62-75.

1183 Barrie, J.V., Conway, K.W., 1999. Late Quaternary glaciation and postglacial
1184 stratigraphy of the northern Pacific margin of Canada. Quat. Res. 123, 113-123.

1185 Barrie, J.V., Conway, K.W., 2002a. Contrasting glacial sedimentation processes and
1186 sea-level changes in town adjacent basins on the Pacific margin of Canada. In:
1187 Dowdeswell, J.A., O'Cofaigh, C. (Eds.), Glacier-influenced Sedimentation on High-
1188 Latitude Continental Margins. Geological Society, London, pp. 181-194.

1189 Barrie, J.V., Conway, K.W., 2002b. Rapid sea-level change and coastal evolution on the
1190 Pacific margin of Canada. Sedimentary Geology 150, 171-183.

1191 Barrie, J.V., Conway, K.W., 2012. Palaeogeographic reconstruction of Hecate Strait
1192 British Columbia: changing sea levels and sedimentary processes reshape a glaciated
1193 shelf. In: Li, M.Z., Sherwood, C.R., Hill, P.R. (Eds.), Sediments, Morphology and
1194 Sedimentary Processes on Continental Shelves: Advances in technologies, research
1195 and applications (Special Publication 44 of the Intl. Assn. Sed.). Wiley-Blackwell,
1196 Chichester.

1197 Barron, J.A., Bukry, D., Dean, W.E., Addison, J.A., Finney, B., 2009. Paleoceanography
1198 of the Gulf of Alaska during the past 15,000 years: Results from diatoms,
1199 silicoflagellates, and geochemistry. Marine Micropaleontology 72, 176-195.

1200 Benson, B.E., Clague, J.J., Grimm, K.A., 1999. Relative sea-level change inferred from
1201 intertidal sediments beneath marshes on Vancouver Island, British Columbia. Quat. Intl.
1202 60, 49-54.

1203 Berthier, E., Schiefer, E., Clarke, G.K.C., Menounos, B., Remy, F., 2010. Contribution of
1204 Alaskan glaciers to sea-level rise derived from satellite imagery. Nature Geosci. 3, 92-
1205 95.

1206 Bobrowsky, P., Clague, J.J., 1992. Neotectonic investigations on Vancouver Island
1207 (92B, F). Paper 1992-1, British Columbia Geological Survey, Paper 1992-1.

1208 Bowles, C.J., Cowgill, E., 2012. Discovering marine terraces using airborne LiDAR
1209 along the Mendocino-Sonoma coast, northern California. Geosphere 8, 386-402.

1210 Byun, S.A., Koop, B.F., Reimchen, T.E., 1997. North American Black Bear mtDNA
1211 phylogeography: implications for morphology and the Haida Gwaii glacial refugium
1212 controversy. Evolution 51, 1647-1653.

1213 Cacchione, D.A., Drake, D.E., Gardner, J.V., 1996. A meandering channel at the base
1214 of the Gorda Escarpment. In: Gardner, J.V., Field, M.E., Twichell, D.C. (Eds.), Geology
1215 of the United States Seaflood: The View from GLORIA. Cambridge University Press, pp.
1216 181-192.

1217 Cannon, A., 2000. Settlement and sea-levels on the central coast of British Columbia:
1218 evidence from shell midden cores. American Antiquity 65, 67-77.

1219 Carlson, P.R., Bruns, T.R., Molnia, B.F., Schwab, W.C., 1982. Submarine valleys in the
1220 northeastern Gulf of Alaska: Characteristics and probable origin. Mar. Geol. 47, 217-
1221 242.

1222 Carlson, P.R., Stevenson, A.J., Bruns, T.R., Mann, D.M., Huggett, W., 1996. Sediment
1223 pathways in Gulf of Alaska from beach to abyssal plain. In: Gardner, J.V., Field, M.E.,
1224 Twichell, D.C. (Eds.), Geology of the United States Seaflood: The View from GLORIA.
1225 Cambridge University Press, pp. 255-278.

1226 Carlson, R.J., 2007. Curretn models for the human colonization of the Americas: the
1227 evidence from Southeast Alaska, 78 pp, Cambridge University.

1228 Carlson, R.L., Bona, L.D., 1996. Early Human Occupation in British Columbia. UBC
1229 Press, Vancouver.

1230 Carrara, P.E., Ager, T.A., Baichtal, J.F., 2007. Possible refugia in the Alexander
1231 Archipelago of southeastern Alaska during the late Wisconsin glaciation. Can. J. Earth
1232 Sci. 44, 229-244.

1233 Church, J.A., White, N.J., 2006. A 20th century acceleration in global sea-level rise.
1234 Geophysical Research Letters 33.

1235 Church, M., Ryder, J.M., 2010. Physiography of British Columbia. In: Pike, R.G.,
1236 Redding, T.E., Moore, R.D., Winkler, R.D., Bladon, K.D. (Eds.), Compendium of Forest
1237 Hydrology and Geomorphology in British Columbia. Ministry of Forests and Range,
1238 Victoria, pp. 17-46.

1239 Cisternas, M., Atwater, B.F., Torrejon, F., Sawai, Y., Machuca, G., Lagos, M., Eipert, A.,
1240 Youlton, C., Salgado, I., Kamataki, T., Shishikura, M., Rajendran, C.P., Malik, J.K.,
1241 Rizal, Y., Husni, M., 2005. Predecessors of the giant 1960 Chile earthquake. Nature
1242 437, 404-407.

1243 Clague, J.J., 1975. Quaternary geology, northern Strait of Georgia. Paper 75-1A.
1244 Geological Survey of Canada, Ottawa, pp. 397-400.

1245 Clague, J.J., 1976. Quadra sand and its relation to the late Wisconsin glaciation of
1246 southwest British Columbia. Can. J. Earth Sci. 13, 803-815.

Clague, J.J., 1981. Late Quaternary geology and geochronology of British Columbia Part 2: summary and discussion of radiocarbon-dated Quaternary history. Paper 80-35, Geological Survey of Canada, Ottawa.

Clague, J.J., 1984. Quaternary geology and geomorphology, Smithers-Terrace-Prince Rupert area, British Columbia. Memoir 413, Geological Survey of Canada, Ottawa.

Clague, J.J., 1989a. Quaternary geology of the Canadian Cordillera (Chapter 1). In: Fulton, R.J. (Ed.), Quaternary Geology of Canada and Greenland. Geological Survey of Canada, Ottawa, pp. 15-96.

Clague, J.J., 1989b. Quaternary geology of the Queen Charlotte Islands, In: Scudder, G.G.E., Gessler, N. (Eds.), The Outer Shores - Proceedings of the Queen Charlotte Islands First International Symposium, University of British Columbia, Vancouver, BC, pp. 65-74.

Clague, J.J., 1989c. Sea levels on Canada's Pacific Coast: Past and future trends. Episodes 12, 29-33.

Clague, J.J., 2003. Canada. In: Bird, E.C.F. (Ed.), The World's Coasts. Springer, Dordrecht, pp. 157-188.

Clague, J.J., Harper, J.R., Hebda, R.J., Howes, D.E., 1982a. Late Quaternary sea levels and crustal movements, coastal British Columbia. Can. J. Earth Sci. 19, 597-618.

Clague, J.J., James, T.S., 2002. History and isostatic effects of the last ice sheet in southern British Columbia. Quat. Sci. Rev. 21, 71-87.

Clague, J.J., Luternauer, J.L., Pullan, S.E., Hunter, J.A., 1991. Postglacial deltaic sediments, southern Fraser River delta, British Columbia. Can. J. Earth Sci. 28, 1386-1393.

Clague, J.J., Mathewes, R.W., Guilbault, J.-P., Hutchinson, I., Ricketts, B.D., 1997. Pre-Younger Dryas resurgence of the southwestern margin of the Cordilleran ice sheet, British Columbia, Canada. Boreas 26, 261-277.

Clague, J.J., Mathewes, R.W., Warner, B.G., 1982b. Late Quaternary geology of eastern Graham Island, Queen Charlotte Islands, British Columbia. Can. J. Earth Sci. 19, 1786-1795.

Clark, J., Mitrovica, J.X., 2011. Regional variability in deglacial sea-level rise across the Oregon-Washington continental shelf: Implications for the archaeological record. INQUA XVIII: Quaternary Sciences - the view from the mountains, Bern, Switzerland.

Clemens, K.E., Komar, P.D., 1988. Oregon beach-sand compositions produced by the mixing of sediments under a transgressing sea. J. Sed. Res. 58, 519-529.

1281 Cohen, S.C., Freymueller, J.T., 1997. Deformation of the Kenai Peninsula, Alaska. J.
1282 Geophys. Res. 102, 20479.

1283 Cohen, S.C., Freymueller, J.T., 2004. Crustal Deformation in the Southcentral Alaska
1284 Subduction Zone. In: Dmowska, R. (Ed.), Advances in Geophysics. Elsevier, San
1285 Diego, pp. 1-63.

1286 Combellick, R.A., 1991. Paleoseismology of the Cook Inlet region, Alaska: Evidence
1287 from peat stratigraphy in Turnagin and Knik Arms. Professional Report 112, Division of
1288 Geological & Geophysical Surveys, Fairbanks.

1289 Dallimore, A., Enkin, R.J., Pienitz, R., Southon, J.R., Baker, J., Wright, C.A., Pedersen,
1290 T.F., Calvert, S.E., Ivanochko, T., Thomson, R.E., 2008. Postglacial evolution of a
1291 Pacific coastal fjord in British Columbia, Canada: interactions of sea-level change,
1292 crustal response, and environmental fluctuations-results from MONA core MD02-2494.
1293 Can. J. Earth Sci. 45, 1345-1362.

1294 Dalrymple, R.A., Breaker, L.C., Brooks, B.A., Cayan, D.R., Griggs, G.B., Han, W.,
1295 Horton, B.P., Hulbe, C.L., McWilliams, J.C., Mote, P.W., Pfeffer, T., Reed, D.J., Shum,
1296 C.K., 2012. Sea-Level Rise for the Coasts of California, Oregon, and Washington: Past,
1297 Present, and Future. The National Academies Press, Washington.

1298 Deschamps, P., Durand, N., Bard, E., Hamelin, B., Camoin, G., Thomas, A.L.,
1299 Henderson, G.M., Okuno, J., Yokoyama, Y., 2012. Ice-sheet collapse and sea-level rise
1300 at the Bolling warming 14,600 years ago. Nature 483, 559-564.

1301 Dethier, D.P., Pessl, F., Keuler, R.F., Balzarini, M.A., Pevear, D.R., 1995. Late
1302 Wisconsinan glaciomarine deposition and isostatic rebound, northern Puget Lowland,
1303 Washington. Geol. Soc. Am. Bull. 107, 1288-1303.

1304 Domingues, C.M., Church, J.A., White, N.J., Gleckler, P.J., Wijffels, S.E., Barker, P.M.,
1305 Dunn, J.R., 2008. Improved estimates of upper-ocean warming and multi-decadal sea-
1306 level rise. Nature 453, 1090-1093.

1307 Doser, D.I., Rodriguez, H., 2011. A seismotectonic study of the Southeastern Alaska
1308 Region. Tectonophysics 497, 105-113.

1309 Easterbrook, D.J., 1963. Late Pleistocene glacial events and relative sea-level changes
1310 in the northern Puget Lowland, Washington. Geol. Soc. Am. Bull. 74, 1465-1483.

1311 Elliott, J.L., Larsen, C.F., Freymueller, J.T., Motyka, R.J., 2010. Tectonic block motion
1312 and glacial isostatic adjustment in southeast Alaska and adjacent Canada constrained
1313 by GPS measurements. J. Geophys. Res. 115, 10.1029/2009jb007139.

1314 Engelhart, S.E., Horton, B.P., Douglas, B.C., Peltier, W.R., Tornqvist, T.E., 2009.
1315 Spatial variability of late Holocene and 20th century sea-level rise along the Atlantic
1316 coast of the United States. Geology 37, 1115-1118.

1317 Fairbanks, R.G., 1989. A 17,000-year glacio-eustatic sea level record: influence of
1318 glacial melting rates on the Younger Dryas event and deep-ocean circulation. Nature
1319 342, 637-642.

1320 Farrell, W.E., Clark, J.A., 1976. On postglacial sea level. Geophys. J. Roy. Astr. Soc.
1321 46, 647-667.

1322 Fedje, D., 1993. Sea-Levels and Prehistory in Gwaii Haanas, 160 pp, University of
1323 Calgary.

1324 Fedje, D., W., Josenhans, H., Clague, J.J., Barrie, J.V., Archer, D.J., Southon, J.R.,
1325 2005. Hecate Strait Paleoshorelines. In: Fedje, D., W., Mathewes, R.W. (Eds.), Haida
1326 Gwaii: Human History And Environment from the Time of Loon to the Time of the Iron
1327 People. UBC Press, Vancouver, pp. 21-37.

1328 Fedje, D.W., Josenhans, H., 2000. Drowned forests and archaeology on the continental
1329 shelf of British Columbia, Canada. Geology 28, 99-102.

1330 Fedje, D.W., Sumpter, I.D., Southon, J.R., 2009. Sea-levels and archaeology in the Gulf
1331 Islands National Park Reserve. Can. J. Arch. 33, 234-253.

1332 Fleming, K., Johnston, P., Zwartz, D., Yokoyama, Y., Lambeck, K., Chappell, J., 1998.
1333 Refining the eustatic sea-level curve since the Last Glacial Maximum using far- and
1334 intermediate-field sites. Earth Plan. Sci. Lett. 163, 327-342.

1335 Freymueller, J.T., Larsen, C.F., Fletcher, H., Echelmeyer, K., Motyka, R.J., 2002. Active
1336 accretion of the Yakutat block to North America. American Geophysical Union, Fall
1337 Meeting, abstract #T12E-02, San Francisco.

1338 Freymueller, J.T., Woodard, H., Cohen, S.C., Cross, R., Elliott, J., Larsen, C.F.,
1339 Hreinsdottir, S., Zweck, C., 2008. Active deformation processes in Alaska, based on 15
1340 years of GPS measurements. In: Freymueller, J.T., Haeussler, P.J., Wesson, R.,
1341 Ekstrom, G. (Eds.), Active Tectonics and Seismic Potential of Alaska, Geophysical
1342 Monograph Series 179. American Geophysical Union, Washington, pp. 1-42.

1343 Friele, P.A., Hutchinson, I., 1993. Holocene sea-level change on the central west coast
1344 of Vancouver Island, British Columbia. Can. J. Earth Sci. 30, 832-840.

1345 Gibson, W.M., 1960. Submarine topography in the Gulf of Alaska. Geol. Soc. Am. Bull.
1346 71, 1087.

1347 Goodbred, S.L., Kuehl, S.A., 2000. The significance of large sediment supply, active
1348 tectonism, and eustasy on margin sequence development: Late Quaternary stratigraphy
1349 and evolution of the Ganges–Brahmaputra delta. Sedimentary Geology 133, 227-248.

1350 Gregoire, L.J., Payne, A.J., Valdes, P.J., 2012. Deglacial rapid sea level rises caused
1351 by ice-sheet saddle collapses. Nature 487, 219-222.

1352 Hamilton, S., Shennan, I., 2005a. Late Holocene great earthquakes and relative sea-
1353 level change at Kenai, southern Alaska. J. Quat. Sci. 20, 95-111.

1354 Hamilton, S., Shennan, I., 2005b. Late Holocene relative sea-level changes and the
1355 earthquake deformation cycle around upper Cook Inlet, Alaska. Quat. Sci. Rev. 24,
1356 1479-1498.

1357 Hampton, M.A., Karl, H.A., Kenyon, N.H., 1989. Sea-floor drainage features of
1358 Cascadia Basin and the adjacent continental slope, northeast Pacific Ocean. Mar. Geol.
1359 87, 249-272.

1360 Heathfield, D.K., Walker, I.J., 2011. Analysis of coastal dune dynamics, shoreline
1361 position, and large woody debris at Wickaninnish Bay, Pacific Rim National Park, British
1362 Columbia. Can. J. Earth Sci. 48, 1185-1198.

1363 Heaton, T.H., Grady, F., 1993. Fossil grizzly bears (Ursus arctos) from Prince of Wales
1364 Island, Alaska, offer new insights into animal dispersal, interspecific competition, and
1365 age of deglaciation. Current Research in the Pleistocene 10, 98-100.

1366 Heaton, T.H., Grady, F., 2003. The Late Wisconsin vertebrate history of Prince of Wales
1367 Island. In: Schubert, B.W., Mead, J.I., Graham, R.W. (Eds.), Ice Age Cave Faunas of
1368 North America. Indiana University Press, Bloomington, pp. 17-53.

1369 Heaton, T.H., Talbot, S.L., Shields, G.F., 1996. An Ice Age refugium for large mammals
1370 in the Alexander Archipelago, southeastern Alaska. Quat. Res. 46, 186-192.

1371 Hetherington, R., Barrie, J.V., Reid, R.G.B., MacLeod, R., Smith, D.J., 2004.
1372 Paleogeography, glacially induced crustal displacement, and Late Quaternary
1373 coastlines on the continental shelf of British Columbia, Canada. Quat. Sci. Rev. 23, 295-
1374 318.

1375 Hetherington, R., Barrie, J.V., Reid, R.G.B., MacLeod, R., Smith, D.J., James, T.S.,
1376 Kung, R., 2003. Late Pleistocene coastal paleogeography of the Queen Charlotte
1377 Islands, British Columbia, Canada, and its implications for terrestrial biogeography and
1378 early postglacial human occupation. Can. J. Earth Sci. 40, 1755-1766.

1379 Hicks, S.D., Shofnos, W., 1965. The determination of land emergence from sea level
1380 observations in Southeast Alaska. J. Geophys. Res. 70, 3315-3320.

1381 Hicock, S.R., Armstrong, J.E., 1985. Vashon drift: definition of the formation in the
1382 Georgia Depression, southwest British Columbia. Can. J. Earth Sci. 22, 748-757.

1383 Holtedahl, H., 1958. Some remarks on geomorphology of continental shelves off
1384 Norway, Labrador, and Southeast Alaska. The Journal of Geology 66, 461-4671.

1385 Horner, R.B., 1983. Seismicity in the St. Elias region of northwestern Canada and
1386 southeastern Alaska. Bull. Seism. Soc. Am. 73, 1117-1137.

1387 Horton, B.P., Shennan, I., 2009. Compaction of Holocene strata and the implications for
1388 relative sealevel change on the east coast of England. Geology 37, 1083-1086.

1389 Howes, D.E., 1981. Late Quaternary history of the Brooks Peninsula, BC Provincial
1390 Museum.

1391 Howes, D.E., 1983. Late Quaternary sediments and geomorphic history of northern
1392 Vancouver Island, British Columbia. Can. J. Earth Sci. 20, 57-65.

1393 Howes, D.E., 1997. Quaternary Geology of Brooks Peninsula. In: Hebda, R.J.,
1394 Haggarty, J.C. (Eds.), Brooks Peninsula: An Ice Age Refugium on Vancouver Island.
1395 BC Ministry of Environment, Lands and Parks, Victoria, pp. 3.1-3.19.

1396 Hutchinson, I., 1992. Holocene sea level change in the Pacific Northwest: a catalogue
1397 of radiocarbon dates and an atlas of regional sea level curves. Occasional Paper No. 1,
1398 Institute for Quaternary Research, Simon Fraser University, Burnaby.

1399 Hutchinson, I., James, T., Clague, J.J., Barrie, J.V., Conway, K., 2004. Reconstruction
1400 of late Quaternary sea-level change in southwestern British Columbia from sediments in
1401 isolation basins. Boreas 33, 183-194.

1402 Hyndman, R.D., Wang, K., 1995. The rupture zone of Cascadia great earthquakes from
1403 current deformation and the thermal regime. J. Geophys. Res. 100, 22133-22154.

1404 Hyndman, R.D., Yorath, C.J., Clowes, R.M., Davis, E.E., 1990. The northern Cascadia
1405 subduction zone at Vancouver Island: seismic structure and tectonic history. Can. J.
1406 Earth Sci. 27, 313-329.

1407 IPCC, 2007. Climate Change 2007: The Physical Science Basis. In: Solomon, S., Qin,
1408 D., Manning, M., Chen, Z., Marquis, M., Averyt, K.B., Tignor, M., Miller, H.L. (Eds.),
1409 Contribution of Working Group 1 to the Fourth Assessment Report of the
1410 Intergovernmental Panel on Climate Change. Cambridge University Press, Cambridge,
1411 UK, and New York, USA, p. 996.

1412 James, T., Rogers, G., Cassidy, J.F., Dragert, H., Hyndman, R.D., Leonard, L.J.,
1413 Nykolaishen, L., Riedel, M., Schmidt, M., Wang, K., 2013. Field studies target 2012
1414 Haida Gwaii earthquake. EOS, Trans. AGU 94, 197-198.

1415 James, T.S., Gowan, E.J., Hutchinson, I., Clague, J.J., Barrie, J.V., Conway, K.W.,
1416 2009a. Sea-level change and paleogeographic reconstructions, southern Vancouver
1417 Island, British Columbia, Canada. Quat. Sci. Rev. 28, 1200-1216.

1418 James, T.S., Gowan, E.J., Wada, I., Wang, K., 2009b. Viscosity of the asthenosphere
1419 from glacial isostatic adjustment and subduction dynamics at the northern Cascadia
1420 subduction zone, British Columbia, Canada. J. Geophys. Res. 114.

James, T.S., Hutchinson, I., Barrie, J.V., Conway, K.W., Mathews, D., 2005. Relative sea-level change in the northern Strait of Georgia, British Columbia. Geog. Phys. et Quat. 59, 113-127.

James, T.S., Hutchinson, I., Clague, J.J., 2002. Improved relative sea-level histories for Victoria and Vancouver, British Columbia, from isolation-basin coring. Current Research 2002-A16, Geological Survey of Canada, Ottawa.

Josenhans, H., Fedje, D., Pienitz, R., Southon, J., 1997. Early humans and rapidly changing Holocene sea levels in the Queen Charlotte Islands-Hecate Strait, British Columbia, Canada. Science 277, 71-74.

Josenhans, H., W., Fedje, D., W., Conway, K.W., Barrie, J.V., 1995. Post glacial sea levels on the Western Canadian continental shelf: evidence for rapid change, extensive subaerial exposure, and early human habitation. Mar. Geol. 125, 73-94.

Kaser, G., Cogley, J.G., Dyurgerov, M.B., Meier, M.F., Ohmura, A., 2006. Mass balance of glaciers and ice caps: Consensus estimates for 1961–2004. Geophysical Research Letters 33, L19501, doi:19510.11029/12006GL027511.

Kaufman, D.S., Manley, W.F., 2004. Pleistocene maximum and late Wisconsinan glacier extents across Alaska, U.S.A. In: Ehlers, J., Gibbard, P.L. (Eds.), Quaternary Glaciations - Extent and Chronology, Part II, North America: Developments in Quaternary Science. Elsevier, pp. 9-27.

Komar, P.D., Allan, J.C., Ruggiero, P., 2011. Sea level variations along the U.S. Pacific Northwest coast: tectonic and climate controls. J. Coastal Res. 27, 808-823.

Kovanen, D.J., Easterbrook, D.J., 2002. Timing and Extent of Allerød and Younger Dryas Age (ca. 12,500–10,000 14C yr B.P.) Oscillations of the Cordilleran Ice Sheet in the Fraser Lowland, Western North America. Quat. Res. 57, 208-224.

Kulm, L.D., Roush, R.C., Harlett, J.C., Neudeck, R.H., Chambers, D.M., Runge, E.J., 1975. Oregon continental shelf sedimentation: Interrelationships of facies distribution and sedimentary processes. The Journal of Geology 83, 145-175.

Lambeck, K., Chappell, J., 2001. Sea level change through the last glacial cycle. Science 292, 679-686.

Larsen, C.F., Motyka, R.J., Freymueller, J.T., Echelmeyer, K.A., Ivins, E.R., 2005. Rapid viscoelastic uplift in southeast Alaska caused by post-Little Ice Age glacial retreat. Earth Plan. Sci. Lett. 237, 548-560.

Lay, T., Ye, L., Kanamori, H., Yamazaki, Y., Cheung, K.F., Kwong, K., Koper, K.D., 2013. The October 28, 2012 Mw 7.8 Haida Gwaii underthrusting earthquake and tsunami: Slip partitioning along the Queen Charlotte Fault transpressional plate boundary. Earth Plan. Sci. Lett. 375, 57-70.

1457 Leonard, L.J., Currie, C.A., Mazzotti, S., Hyndman, R.D., 2010. Rupture area and
1458 displacement of past Cascadia great earthquakes from coastal coseismic subsidence.
1459 Geol. Soc. Am. Bull. 122, 2079-2096.

1460 Leonard, L.J., Hyndman, R.D., Mazzotti, S., 2004. Coseismic subsidence in the 1700
1461 great Cascadia earthquake: Coastal estimates versus elastic dislocation models. Geol.
1462 Soc. Am. Bull. 116, 655.

1463 Linden, R.H., Schurer, P.J., 1988. Sediment characteristics and sea-level history of
1464 Royal Roads Anchorage, Victoria, British Columbia. Can. J. Earth Sci. 25, 1800-1810.

1465 Litchfield, N.J., Lian, O.B., 2004. Luminescence age estimates of Pleistocene marine
1466 terrace and alluvial fan sediments associated with tectonic activity along coastal Otago,
1467 New Zealand. NZ J. Geol. Geophys. 47, 29-37.

1468 Long, A.J., Shennan, I., 1994. Sea-level changes in Washington and Oregon and the
1469 "earthquake deformation cycle". J. Coastal Res. 10, 825-838.

1470 Long, A.J., Shennan, I., 1998. Models of rapid relative sea-level change in Washington
1471 and Oregon, USA. The Holocene 8, 129-142.

1472 Luternauer, J.L., Clague, J.J., Conway, K.W., Barrie, J.V., Blaise, B., Mathewes, R.W.,
1473 1989a. Late Pleistocene terrestrial deposits on the continental shelf of western Canada
1474 - evidence for rapid sea-level change at the end of the last glaciation. Geology 17, 357-
1475 360.

1476 Luternauer, J.L., Conway, K.W., Clague, J.J., Blaise, B., 1989b. Late Quaternary
1477 geology and geochronology of the central continental shelf of western Canada. Mar.
1478 Geol. 89, 57-68.

1479 Mann, D.H., 1986. Wisconsin and Holocene glaciation in southeast Alaska. In:
1480 Hamilton, T.D., Reed, K.M., Thorson, R.M. (Eds.), Glaciation in Alaska: the Geologic
1481 Record. Alaska Geological Society, Anchorage, pp. 237-265.

1482 Mann, D.H., Hamilton, T.D., 1995. Late Pleistocene and Holocene paleoenvironments
1483 of the North Pacific coast. Quat. Sci. Rev. 14, 449-471.

1484 Mann, D.H., Peteet, D.M., 1994. Extent and timing of the last glacial maximum in
1485 southwestern Alaska. Quat. Res. 42, 136-148.

1486 Mann, D.H., Streveler, G.P., 2008. Post-glacial relative sea level, isostasy, and glacial
1487 history in Icy Strait, Southeast Alaska, USA. Quat. Res. 69, 201-216.

1488 Mathews, W.H., 1991. Ice sheets and ice streams: thoughts on the Cordilleran Ice
1489 Sheet symposium. Geog. Phys. et Quat. 45, 263-267.

1490 Mathews, W.H., Fyles, J.G., Nasmith, H.W., 1970. Postglacial crustal movements in
1491 southwestern British Columbia and adjacent Washington state. Can. J. Earth Sci. 7,
1492 690-702.

1493 Mauz, B., Hijma, M.P., Amorosi, A., Porat, N., Galili, E., Bloemendal, J., 2013. Aeolian
1494 beach ridges and their significance for climate and sea level: Concept and insight from
1495 the Levant coast (East Mediterranean). Earth-Sci. Rev. 121, 31-54.

1496 Mazzotti, S., Dragert, H., Henton, J., Schmidt, M., Hyndman, R., James, T., Lu, Y.,
1497 Craymer, M., 2003. Current tectonics of northern Cascadia from a decade of GPS
1498 measurements. J. Geophys. Res. 108, 2554.

1499 Mazzotti, S., Jones, C., Thomson, R.E., 2008. Relative and absolute sea level rise in
1500 western Canada and northwestern United States from a combined tide gauge-GPS
1501 analysis. J. Geophys. Res. 113, C11019.

1502 Mazzotti, S., Lambert, A., Van der Kooij, M., Mainville, A., 2009. Impact of
1503 anthropogenic subsidence on relative sea-level rise in the Fraser River delta. Geology
1504 37, 771-774.

1505 McKenzie, G.D., Goldthwait, R.P., 1971. Glacial history of the last eleven thousand
1506 years in Adams Inlet, southeastern Alaska. Geol. Soc. Am. Bull. 82, 1767-1782.

1507 McLaren, D., Fedje, D., Hay, M., Mackie, Q., Walker, I.J., Shugar, D.H., Eamer, J.B.R.,
1508 Lian, O.B., Neudorf, C., In review. A post-glacial sea level hinge on the central Pacific
1509 coast of Canada. Quat. Sci. Rev. Submission ID JQSR-D-14-00035.

1510 McLaren, D., Martindale, A., DFedje, D., Mackie, Q., 2011. Relict shorelines and shell
1511 middens of the Dundas Archipelago. Can. J. Arch. 35, 86-116.

1512 Milne, G.A., Gehrels, W.R., Hughes, C.W., Tamisiea, M.E., 2009. Identifying the causes
1513 of sea-level change. Nature Geosci. 2, 471-478.

1514 Mobley, C.M., 1988. Holocene sea levels in southeast Alaska: preliminary results. Arctic
1515 41, 261-266.

1516 Molnia, B.F., Post, A., 1995. Holocene history of Bering Glacier, Alaska: a prelude to the
1517 1993–1994 surge. Phys. Geog. 16, 87-117.

1518 Mosher, D.C., Hewitt, A.T., 2004. Late Quaternary deglaciation and sea-level history of
1519 eastern Juan de Fuca Strait, Cascadia. Quat. Intl. 121, 23-39.

1520 Motyka, R.J., 2003. Little Ice Age subsidence and post Little Ice Age uplift at Juneau,
1521 Alaska, inferred from dendrochronology and geomorphology. Quat. Res. 59, 300-309.

1522 Motyka, R.J., Echelmeyer, K., 2003. Taku Glacier (Alaska, U.S.A.) on the move again:
1523 active deformation of proglacial sediments. J. Glaciol. 49, 50-58.

1524 Nelson, A.R., 2007. Tectonics and relative sea-level change: tectonic locations. In:
1525 Elias, S.A. (Ed.). Elsevier, Encyclopedia of Quaternary Science, pp. 3072-3087.

1526 Nelson, A.R., Jennings, A.E., Kashima, K., 1996a. An earthquake history derived from
1527 stratigraphic and microfossil evidence of relative sea-level change at Coos Bay,
1528 southern coastal Oregon. Geol. Soc. Am. Bull. 108, 141-154.

1529 Nelson, A.R., Kashima, K., 1993. Diatom Zonation in Southern Oregon Tidal Marshes
1530 Relative to Vascular Plants, Foraminifera, and Sea Level. J. Coastal Res. 9, 673-697.

1531 Nelson, A.R., Kelsey, H.M., Witter, R.C., 2006. Great earthquakes of variable
1532 magnitude at the Cascadia subduction zone. Quat. Res. 65, 354-365.

1533 Nelson, A.R., Sawai, Y., Jennings, A.E., Bradley, L.-A., Gerson, L., Sherrod, B.L.,
1534 Sabean, J., Horton, B.P., 2008. Great-earthquake paleogeodesy and tsunamis of the
1535 past 2000 years at Alsea Bay, central Oregon coast, USA. Quat. Sci. Rev. 27, 747-768.

1536 Nelson, A.R., Shennan, I., Long, A.J., 1996b. Identifying coseismic subsidence in tidal-
1537 wetland stratigraphic sequences at the Cascadia subduction zone of western North
1538 America. J. Geophys. Res. 101, 6115-6135.

1539 Nishenko, S.P., Jacob, K.H., 1990. Seismic potential of the Queen Charlotte-Alaska-
1540 Aleutian Seismic Zone. J. Geophys. Res. 95, 2511.

1541 Nittrouer, J.A., Best, J.L., Brantley, C., Cash, R.W., Czapiga, M., Kumar, P., Parker, G.,
1542 2012. Mitigating land loss in coastal Louisiana by controlled diversion of Mississippi
1543 River sand. Nature Geosci. 5, 534-537.

1544 Nittrouer, J.A., Viparelli, E., 2014. Sand as a stable and sustainable resource for
1545 nourishing the Mississippi River delta. Nature Geosci. 7, 350-354.

1546 Ovenshine, A.T., Lawson, D.E., Bartsch-Winkler, S.R., 1976. The Placer River silt - an
1547 intertidal deposit caused by the 1964 Alaska earthquake. U.S. Geological Survey J.
1548 Res. 4, 151-162.

1549 Peltier, W.R., 2002. On eustatic sea level history: Last Glacial Maximum to Holocene.
1550 Quat. Sci. Rev. 21, 377-396.

1551 Peteet, D.M., 2007. Muskeg archives of vegetation, migration, and climate history in the
1552 Gulf of Alaska arc. Geological Society of America, Cordilleran Section - 103rd Annual
1553 Meeting, Bellingham.

1554 Péwé, T.L., 1975. Quaternary Geology of Alaska. Professional Paper 835, U.S.
1555 Geological Survey, Washington.

1556 Plafker, G., 1969. Tectonics of the March 27, 1964, Alaska earthquake. Professional
1557 Paper 543-I, U.S. Geological Survey, Washington.

1558 Plafker, G., 1990. Regional vertical tectonic displacement of shorelines in south-central
1559 Alaska during and between great earthquakes. Northwest Science 64, 250-258.

1560 Plafker, G., Hudson, T., Rubin, C.M., Dixon, K.L., 1981. Holocene marine terraces and
1561 uplift history in the Yakataga seismic gap near Icy Cape, Alaska. In: Coonrad, W.L.
1562 (Ed.), The United States Geological Survey in Alaska: Accomplishments during 1980;
1563 Circular 844. U.S. Geological Survey, Washington, pp. 111-115.

1564 Plafker, G., Rubin, C.M., 1978. Uplift history and earthquake recurrence as deduced
1565 from marine terraces on Middleton Island, Alaska. Open File 78-943; Proceedings of
1566 Conference VI, Methodology for identifying seismic gaps and soon-to-break gaps. U.S.
1567 Geological Survey, Washington, pp. 687-721.

1568 Plafker, G., Savage, J.C., 1970. Mechanism of the Chilean Earthquakes of May 21 and
1569 22, 1960. Geol. Soc. Am. Bull. 81, 1001-1030.

1570 Porter, S.C., Swanson, T.W., 1998. Radiocarbon age constraints on rates of advance
1571 and retreat of the Puget Lobe of the Cordilleran Ice Sheet during the last glaciation.
1572 Quat. Res. 50, 205-213.

1573 Reger, R.D., Pinney, D.S., 1995. Late Wisconsin glaciation of the Cook Inlet region with
1574 emphasis on Kenai Lowland and implications for early peopling. In: Davis, N.Y., Davis,
1575 W.E. (Eds.), Adventures Through Time: readings in the Anthropology of Cook Inlet,
1576 Alaska. Cook Inlet Historical Society, Anchorage, pp. 13-36.

1577 Reimchen, T.E., Byun, S.A., 2005. The evolution of endemic species on Haida Gwaii.
1578 In: Fedje, D., W., Mathewes, R.W. (Eds.), Haida Gwaii: Human History And
1579 Environment from the Time of Loon to the Time of the Iron People Vancouver, pp. 77-
1580 95.

1581 Retherford, R.M., 1970. Late Quaternary geologic ewnvironments and their relation to
1582 archaeological studies in the Bella Bella-Bella Coola region of the British Columbia
1583 coast, 128 pp, University of Colorado at Boulder, Boulder.

1584 Riddihough, R.P., 1982. Contemporary movements and tectonics on Canada's west
1585 coast: a discussion. Tectonophysics 86, 319-341.

1586 Rink, W.J., López, G.I., 2010. OSL-based lateral progradation and aeolian sediment
1587 accumulation rates for the Apalachicola Barrier Island Complex, North Gulf of Mexico,
1588 Florida. Geomorphology 123, 330-342.

1589 Roe, H.M., Doherty, C.T., Patterson, R.T., Milne, G.A., 2013. Isolation basin records of
1590 late Quaternary sea-level change, central mainland British Columbia, Canada. Quat.
1591 Intl.

1592 Rogers, G., Dragert, H., 2003. Episodic tremor and slip on the Cascadia subduction
1593 zone: The chatter of silent slip. Science 300, 1942-1943.

1594 Rubin, M., Alexander, C., 1958. U.S. Geological Survey radiocarbon dates iV. Science
1595 127, 1476-1487.

1596 Sato, T., Larsen, C.F., Miura, S., Ohta, Y., Fujimoto, H., Sun, W., Motyka, R.J.,
1597 Freymueller, J.T., 2011. Reevaluation of the viscoelastic and elastic responses to the
1598 past and present-day ice changes in Southeast Alaska. Tectonophysics 511, 79-88.

1599 Savage, J.C., Plafker, G., 1991. Tide gage measurements of uplift along the south coast
1600 of Alaska. J. Geophys. Res. 96, 4325-4335.

1601 Savage, J.C., Thatcher, W., 1992. Interseismic deformation at the Nankai Trough,
1602 Japan, subduction zone. J. Geophys. Res. 97, 11117-11135.

1603 Schmoll, H.R., Szabo, B.J., Rubin, M., Dobrovolny, E., 1972. Radiometric Dating of
1604 Marine Shells from the Bootlegger Cove Clay, Anchorage Area, Alaska. Geol. Soc. Am.
1605 Bull. 83, 1107-1114.

1606 Shennan, I., 1986. Flandrian sea-level changes in the Fenland. II: Tendencies of sea-
1607 level movement, altitudinal changes, and local and regional factors. J. Quat. Sci. 1, 155-
1608 179.

1609 Shennan, I., 2009. Late Quaternary sea-level changes and palaeoseismology of the
1610 Bering Glacier region, Alaska. Quat. Sci. Rev. 28, 1762-1773.

1611 Shennan, I., Bradley, S., Milne, G., Brooks, A., Bassett, S., Hamilton, S., 2006. Relative
1612 sea-level changes, glacial isostatic modelling and ice-sheet reconstructions from the
1613 British Isles since the Last Glacial Maximum. J. Quat. Sci. 21, 585-599.

1614 Shennan, I., Hamilton, S., 2006. Coseismic and pre-seismic subsidence associated with
1615 great earthquakes in Alaska. Quat. Sci. Rev. 25, 1-8.

1616 Shennan, I., Horton, B., 2002. Holocene land- and sea-level changes in Great Britain. J.
1617 Quat. Sci. 17, 511-526.

1618 Sirkin, L.A., Tuthill, S.J., 1969. Late Pleistocene palynology and stratigraphy of
1619 Controller Bay region, Gulf of Alaska, In: Ters, M. (Ed.), Etudes sur le Quaternaire dans
1620 le Monde: 8th INQUA Congress, Paris, pp. 197-208.

1621 Smith, D.E., Harrison, S., Firth, C.R., Jordan, J.T., 2011. The early Holocene sea level
1622 rise. Quat. Sci. Rev. 30, 1846-1860.

1623 Stuiver, M., Reimer, P.J., Reimer, R.W., 2013. Calib 7.0. http://www.calib.org
1624 14CHRONO Centre, Queen's University Belfast, Belfast. [Accessed October 1, 2013].

1625 Szeliga, W., 2013. 2012 Haida Gwaii quake: insight into Cascadia's subduction extent.
1626 EOS, Trans. AGU 94, 85-96.

1627 Thatcher, W., 1984. The earthquake deformation cycle at the Nankai Trough, southwest
1628 Japan. J. Geophys. Res. 89, 3087-3101.

1629 Valentine, K.W.G., 1971. Soils of the Tofino-Ucluelet lowland of British Columbia.
1630 Canada Department of Agriculture, British Columbia Soil Survey, Report No. 11,
1631 Canada Department of Agriculture, Ottawa.

1632 Ward, B.C., Wilson, M.C., Nagorsen, D.W., Nelson, D.E., Driver, J.C., Wigen, R.J.,
1633 2003. Port Eliza cave: North American West Coast interstadial environment and
1634 implications for human migrations. Quat. Sci. Rev. 22, 1383-1388.

1635 Warner, B.G., Mathewes, R.W., Clague, J.J., 1982. Ice-free conditions on the Queen
1636 Charlotte Islands, British Columbia, at the height of late Wisconsinan glaciation. Science
1637 218, 675-677.

1638 Weaver, A.J., Saenko, O.A., Clark, P.U., Mitrovica, J.X., 2003. Meltwater pulse 1A from
1639 Antarctica as a trigger of the Bolling-Allerod warm interval. Science 299, 1709-1713.

1640 Williams, H.F.L., Roberts, M.C., 1989. Holocene sea-level change and delta growth -
1641 Fraser River delta, British Columbia. Can. J. Earth Sci. 26, 1657-1666.

1642 Witter, R.C., Kelsey, H.M., Hemphill-Haley, E., 2003. Great Cascadia earthquakes and
1643 tsunamis of the past 6700 years, Coquille River estuary, southern coastal Oregon. Geol.
1644 Soc. Am. Bull. 115, 1289-1306.

1645 Wolfe, S.A., Walker, I.J., Huntley, D.J., 2008. Holocene coastal reconstruction, Naikoon
1646 peninsula, Queen Charlotte Islands, British Columbia. Current Research 2008-12,
1647 Geological Survey of Canada, Ottawa.
1648